8090

NAME OF AUTHOR....*Edward Karpinski*........

TITLE OF THESIS...*Measurement of Vasodilatation in the submaxillary gland of the cat*....

UNIVERSITY........*Alberta*....................

DEGREE FOR WHICH THESIS WAS PRESENTED....*Ph. D.*........

YEAR THIS DEGREE GRANTED........*1971*..............

(Signed)*Edward Karpinski*........

PERMANENT ADDRESS:

....*7737-83 Ave*....

....*Edmonton*........

....

DATED *Jul. 19*............19 7/

THE UNIVERSITY OF ALBERTA

MEASUREMENT OF VASODILATATION IN

THE SUBMAXILLARY GLAND OF THE CAT

by

© Edward Karpinski

A THESIS

SUBMITTED TO THE FACULTY OF GRADUATE STUDIES

IN PARTIAL FULFILMENT OF THE REQUIREMENTS FOR THE DEGREE

OF DOCTOR OF PHILOSOPHY

DEPARTMENTS OF PHYSIOLOGY

AND ELECTRICAL ENGINEERING

EDMONTON, ALBERTA

SPRING, 1971

UNIVERSITY OF ALBERTA

FACULTY OF GRADUATE STUDIES

The undersigned certify that they have read, and
recommend to the Faculty of Graduate Studies for accep-
tance, a thesis entitled "Measurement of Vasodilatation
in the Submaxillary Gland of the Cat" submitted by Edward
Karpinski in partial fulfillment of the requirements for
the degree of Doctor of Philosophy.

.....R. Bitten.........
Acting Supervisor

.....W.A. Kingma......
Co-supervisor

.....Susanne Barton.....

....

R. Rink

.....F.C. Macintosh.....
External Examiner

Date..January 25, 1971   ....

ACKNOWLEDGMENTS

ABSTRACT

A new flow meter has been designed and developed to
measure the venous outflow from the submaxillary gland of
the cat. The flow meter is of the thermal type and measures
a wide range of venous flows. The sensing device is a
thermistor which is kept at a constant temperature by
feedback of electrical power and this change in power gives
a measure of fluid velocity which is independent of
thermistor characteristics. A second thermistor is used
as a reference to provide corrections for temperature
changes in the fluid and to provide a balance for zero
velocity. The flow meter has been applied to the study of
vasodilatation in the submaxillary gland of the cat. Its
rapid response to changes in venous outflow on parasympath-
etic nerve stimulation enables the detection of vasodilata-
tion in less than one half of a second after nerve stimula-
tion. The latency between parasympathetic nerve stimula-
tion and hyperpolarization of secretory cells is approxi-
mately the same as that of vasodilatation. This would
support the direct innervation of the vasculature by nerve
fibers rather than a metabolic vasodilator such as the
kallikrein-kinin system.

Table of Contents

List of Figures

List of Tables

List of Symbols

α	temperature coefficient of resistance in a thermistor.
B	magnetic field strength.
β	constant depending on thermistor material (4000).
C_p	specific heat of the fluid at constant pressure.
C	heat capacity of the thermistor
D	thermal diffusivity of the fluid in cm^2/sec.
∇	vector operator.
δ	boundary layer (velocity).
e_o	output voltage.
E	electric field strength.
G_1---G_n	transfer functions.
H	transfer function.
κ	thermal conductivity of the fluid milliwatts/cm.
K---K_n	static gain constants.
K(v)	dissipation factor.
Nu	Nusselt nember (dimensionless heat transfer coefficient).
θ	spherical co-ordinate.
P	power in milliwatts.
ρ	density of the fluid in gm/cm^3.
Pr	Prandtl number.
Re	Reynold's number.
r_o	radius of thermistor.
r	spherical co-ordinate.

R	resistance.
R_0	initial resistance.
s	Laplace transform.
ΔT	temperature difference.
T	temperature.
$\tau \text{---} \tau_n$	time constants.
t	time.
ν	Kinematic viscosity.
V	velocity.

Chapter 1   MEASUREMENT OF BLOOD FLOW

1.1 Introduction

Blood flow measurement techniques are numerous and
are worthy of being called a highly developed science.
This science has developed as an off-shoot from techniques
developed by physicists and engineers used to measure the
flow of fluids. The techniques for measuring blood flow
are, of course, modifications due to the unique problems
encountered when attempting to measure blood flow in
humans and in undisturbed experimental animals. The main
techniques in use are clearance methods, electromagnetic
and ultrasonic flow meter methods. (The clearance methods
are direct applications of the Fick principle which states
that the blood flow through a gland or organ is the amount
of substance cleared per unit of time divided by the
arteriovenous concentration difference produced by this
clearance.) Other methods are the heated thermocouple, or
thermistor, and the drop counter. These latter methods
are very sensitive but, with the exception of the drop
counter, are difficult to calibrate. Another technique is
plethysmography, which measures volume changes in a limb
or an organ. It does not however separate the flows in
the various tissues of the limb.

In physiology a problem may be the control of blood
flow to an organ or gland, so that the knowledge of sudden
changes in blood flow in one vessel is important. The

useful techniques in this case are then limited. One can

not, for example, use a clearance technique since it would

not show rapid changes. Plethysmography could be used but

is usually very difficult to apply to a whole gland or

organ, and if water is used as the surrounding fluid it

would damp out any rapid changes in flow.

Other techniques which could be used employ the

following:

(1) electromagnetic flow meter

(2) ultrasonic flow meter

(3) drop counter

(4) heated thermistor or thermocouple.

1.2 Electromagnetic Flow Meter

The correct name for this type of flow meter is the

electromagnetic induction flow meter. The principle behind

it is described by Faraday's Law which states that an

electrical potential will be developed across a conductor

(blood) moving through a magnetic field. The magnitude of

the electrical potential induced is proportional to the

magnetic field strength and the velocity of the moving

conductor.

$$E \propto BV \qquad \ldots(1.1)$$

where B = magnetic field strength and

V = velocity.

If the conductor is circular and the velocity profile

is axially symmetrical, the induced voltage is proportional to the average velocity.

In practice, the electromagnet is driven by either a sine wave or a square wave of current. This presents problems since the electrodes and wires leading from the electrodes form the secondary of a transformer; the primary being the driving coil of the electromagnet. This quadrature voltage may be larger than the flow induced voltage. Several methods are used which overcome this problem. The most popular is one in which the electromagnet is driven by a fairly high frequency square wave and the induced voltage is sampled when the rate of change of the applied field is zero.

1.3 Ultrasonic Flow Meter

The ultrasonic technique consists of two methods. One method is based on the physical phenomenon that the effective velocity of sound through a moving medium is the sum of the velocity of sound relative to the medium and the velocity of the medium. The other method which is much simpler to apply, is the Doppler Shift sonic flow meter method. When a sound wave is reflected from a moving target, the frequency of the reflected sound differs from the frequency of the incident sound by a quantity proportional to the velocity of the target relative to the sound source. This type of flow meter is easy to build and is accurate to a very low flow range, but it does not discrim-

inate the direction of flow.

1.4 Drop Counter

The drop counter counts drops of blood via a light and photocell arrangement while a rate meter or recorder records the flow. It is useful for small flows but its disadvantages are speed of response, and the fact that some arrangement must be made to put the blood back into the animal. Also when the flow is high it cannot distinguish between drops.

1.5 Heated Thermocouple or Thermistor

The heated thermocouple or thermistor principle is usually based on the fact that the elements are heated above the temperature of the blood. Blood flow past the heated element cools it by forced convection. Changes in temperature are detected by bridge arrangements and give indications of the flow rate. Another application is one in which the heated element detects the changes in thermal conductivity of the tissue as a result of changes in blood flow. These methods are usually slow because of the thermal time constants of the elements and, since they are non-linear, they are very difficult to calibrate. They are however, very sensitive and will measure very small velocities.

Chapter 2   FORCED CONVECTION FLOW METER

2.1 Summary of Methods

The problem of measuring flows to and from glands
and organs is partially solved. For example, if the flow
is greater than several cc./min., and is arterial, electro-
magnetic or ultrasonic techniques can be employed. If the
flow is small and venous, the only linear instrument which
can be used is the drop counter. However there are diffi-
culties with its speed of response as it responds very
slowly. In order to study the control of blood flow to the
submaxillary gland of the cat, where basal flows are of the
order of 0.25 to 1.0 cc. per minute and the arterial supply
is very diffuse and inaccessible, a new technique for flow
measurement had to be developed.

2.2 General Specifications of Flow Meter

Since high sensitivities are required, this indicates
that a thermal technique would be the most plausible, for
example, a heated thermocouple or thermistor. Thermal
devices are very sensitive and are the most useful form of
transducer capable of measuring the low velocities involved
in venous outflows from glands. Since thermistors can be
made very small, they are the logical choice for the sensor.
Also, their thermal times are quite small. The bandwidth
of a thermistor sensor, as is done in hot wire anemometry,
may be increased by supplying feedback as has been attempted

by Katsura, Weiss, Baker and Rushmer (1959) and Grahn, Paul
and Wessel (1968). The thermistor, in order to eliminate
thermal delays and to improve the speed of response, must
be in the flow stream whereas the probe, to compensate for
changes in blood temperature, must have two thermistors--
one which measures the flow and one which compensates for
the minute temperature changes of the blood.

Several possibilities exist for the placement of the
thermistor:

    (1)   at the end of a flexible catheter

    (2)   inside a needle

    (3)   inside a rigid tube which, through a double
        cannulation, becomes part of the blood
        vessel.

For the particular application in mind (the venous
outflow from the submaxillary gland) the latter method was
chosen due to the size of the vessel and the location in
the animal.

2.3 Thermistor

The detecting element of the flow meter is a thermistor
which is a semi-conductor of ceramic material. It is made
by sintering mixtures of metallic oxides such as manganese,
nickel, cobalt, copper, iron and uranium. Thermistors are
resistors with a high negative temperature coefficient of
resistance. As the temperature increases, the resistance
decreases. The mathematical expression which relates the

resistance and absolute temperature of the thermistor is
as follows:

$$R_0(T) = R_0(T_0)e^{\beta(\frac{1}{T} - \frac{1}{T_0})} \qquad \ldots(2.1)$$

where $R_0(T)$ = the resistance at absolute temperature T

$R_0(T_0)$ = the resistance at absolute temperature

T_0 and

β = a constant which depends on the material used

to make the thermistor.

Equation 2.1 applies to an indirectly heated thermistor;
one in which no power is being dissipated.

2.4 Self-Heated Thermistor

If a very small voltage is applied to a thermistor, a
small current will flow which does not produce enough heat
in the thermistor to heat it measurably above its surround-
ings. Under these circumstances, Ohm's Law will be follow-
ed and the current will be proportional to the applied
voltage. However, if the voltage is gradually increased,
the current will increase and the heat generated in the
thermistor will raise its temperature above that of its
surroundings. The resistance will consequently be lowered
and more current will flow. Figure 1 shows that the voltage
drop across a thermistor (Fenwal BC32L1) increases as the
current increases until it reaches a peak value beyond
which the voltage drop decreases as the current further
increases. In the latter portion of the curve the thermistor

is exhibiting a negative resistance characteristic. Figure
1 shows the characteristics of a BC32L1 thermistor at two
fluid temperatures--19.5 and 37° C.

Thermistor type BC32L1

Thermistor voltage (V)

Thermistor current (mA)

19.5°C

37°C
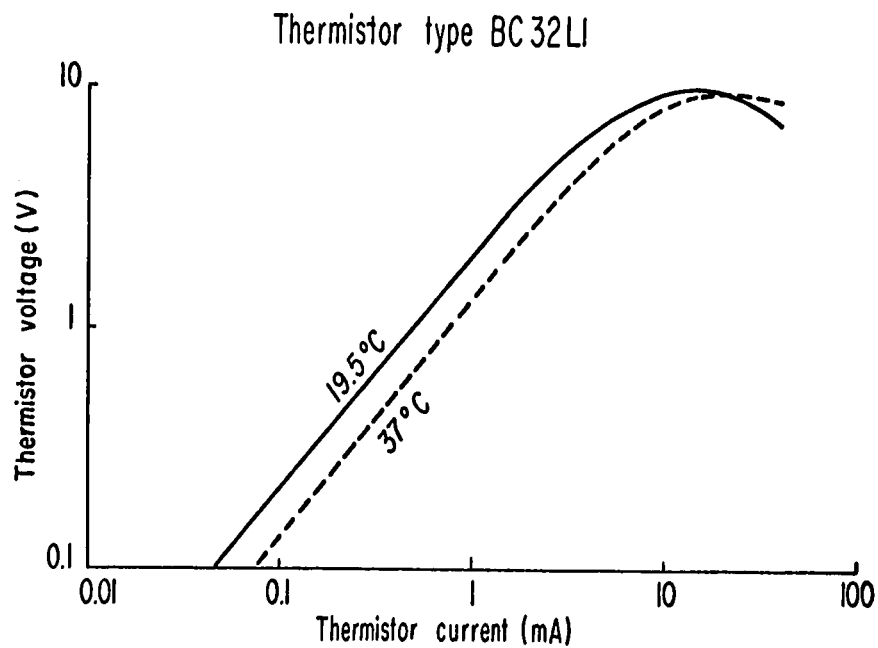
Figure 1. Steady state voltage current characteristics of
a Fenwal BC32L1 thermistor at fluid temperatures of 19.5
and 37° C. The fluid is 0.16M saline.

The self-heated thermistor situated in a fluid is
cooled by heat conduction, free and forced convection and
radiation. It is generally accepted that radiation effects
may be neglected if the temperature difference between the

fluid and thermistor is small (Hinze, 1959). Free convection effects are independent of fluid velocity. The total amount of heat transferred from a self-heated thermistor to the fluid due to forced convection depends upon:

    (1)   flow velocity

    (2)   the difference in temperature between the thermistor and the fluid

    (3)   the physical properties of the fluid

    (4)   the dimensions and physical properties of the thermistor.

2.5 Probe

The probe was made of a thin wall glass tube. The probe diameters were chosen to fit various sizes of blood vessels. Glass tubing was used so that the thermistor leads could be soldered to the tubing. This was done in order to overcome the difficulty encountered in attaching leads to the thermistor leads. The thermistor leads are 0.001 inch platinum iridium wire. The bead is approximately 0.007 inch with a specified resistance of 2 kilo-ohms at 20° C. To construct the probe, holes were drilled in the glass tube at right angles 0.5 mm. apart and 0.25 mm. in diameter. Figure 2 shows the glass tube used in a typical probe.

Two thermistors were inserted into the probe and were staggered off center to prevent one thermistor from blocking the flow to the other one. The thermistor leads were

attached to the tubing by painting with conducting epoxy.

To this epoxy long wire leads were soldered. The 0.25 mm.

holes through which thermistor leads passed were completely

plugged with silicone rubber and the long wire leads were

then epoxied onto the glass with conventional epoxy to give

a good mechanical contact. The epoxy was then coated with

a thin layer of silicone rubber in order to make it resis-

tant to moisture. Figure 3 shows the approximate location

of the two thermistors in the glass tube.
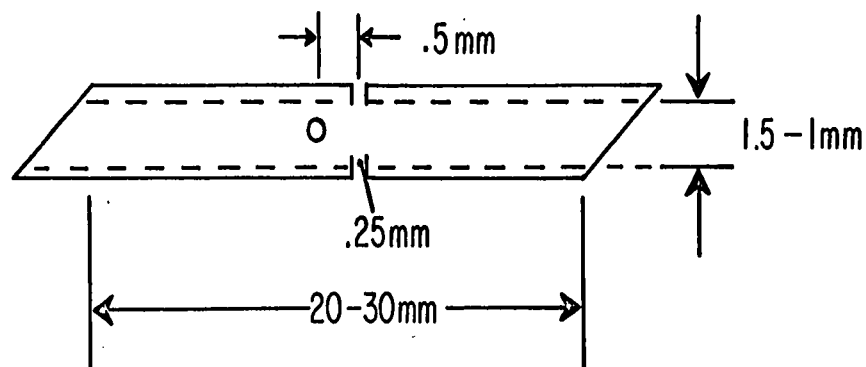
Figure 2. Glass tube used for probe (not to scale).

−silicone rubber plugs
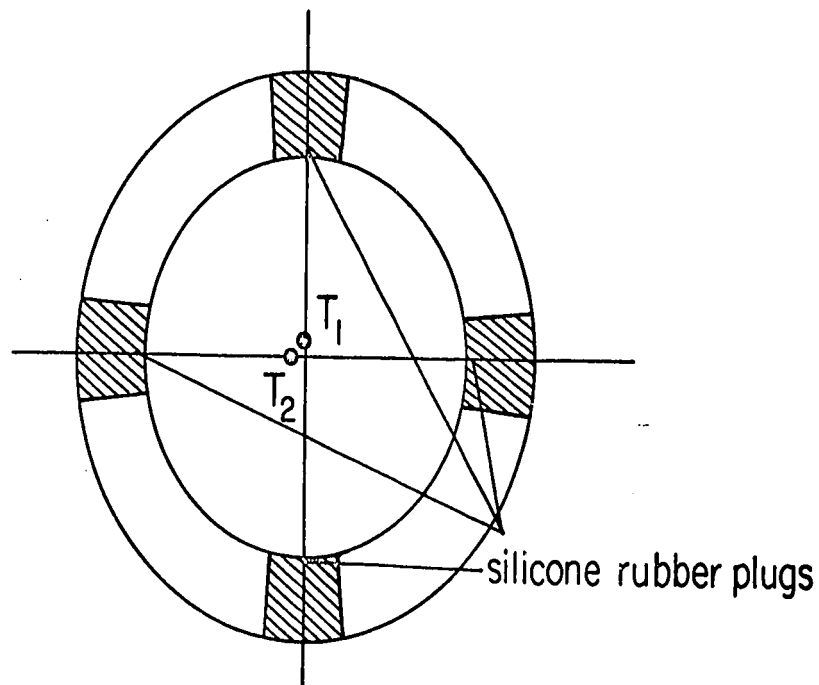
Figure 3. Approximate location of the two thermistors in the glass tube.

2.6 Flow Meter Scheme

The general scheme of a flow meter using thermistors falls into two categories:

(1) constant current

(2) constant temperature.

For this project the constant temperature technique was chosen in order to decrease the time constant of the thermistor. This technique consists of a scheme in which the power is adjusted automatically using negative feed-

back to keep the temperature, and hence the resistance of the measuring thermistor, constant. This system works well for hot wires, and simple D.C. systems may be designed. However, in the case of thermistors with their high negative temperature coefficients of resistance, a D.C. system results in an inherently unstable positive feedback system. Grahn, Paul and Wessel (1968, 1969) claim they have achieved stability and speed with a D.C. system. An evaluation of the system used by Grahn, Paul and Wessel indicates that the system gain is less than unity. This would result in their achieved stability but it leaves in doubt their claim for improved system bandwidth.

In this project a technique originally suggested by Ziegler (1934) was used. He suggested that the heating current and the error voltage be separated. In a system which measures the resistance of the thermal sensor by means of D.C. and which heats the sensor by means of RF power, one can obtain such a system in which heating does not influence the measurement. Such a system has never been designed. The scheme suggested by Ziegler to improve the stability of hot wire systems, is essential for a thermistor system because of the negative temperature coefficient of resistance of thermistors.

The system used in this project consisted of a high frequency oscillator which was amplitude modulated. The amplitude modulator drives a power amplifier which in turn drives the thermistor. A D.C. bias current through

the thermistor is used to indicate changes in resistance.

This change in resistance causes the error voltage which is

amplified and in turn changes the amount of RF power fed

into the thermistor. The output voltage of the amplifier

is then a function of velocity. Figure 4 is a basic scheme

of the proposed forced convection flow meter.
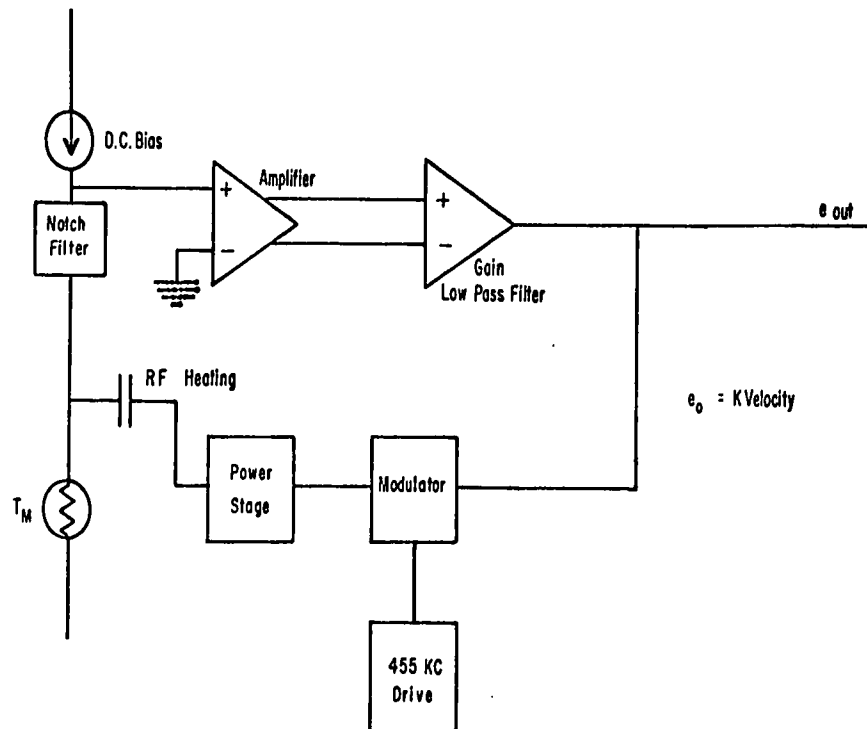
Figure 4. Basic scheme of flow meter.

2.7 Thermistor Biasing

The measuring thermistor must be heated above the ambient temperature of the fluid so that it is sensitive to velocity. This requires some bias power. The bias power must be large enough so that the thermistor is in the self-heated portion of its characteristic but not so large that it is in the negative resistance portion of its characteristic (Figure 1). The temperature of the thermistor in this case must also be below the temperature that would cause damage to the blood.

Chapter 3   STEADY STATE RESPONSE OF FLOW METER

3.1   Introduction

If a heated body such as a thermistor is placed in a
fluid stream and kept at a constant temperature above the
ambient temperature of the fluid, power is required to
maintain it at that temperature. This power depends on the
fluid velocity, the specific heat of the fluid, the temper-
ature difference and the thermal conductivity of the fluid.
Therefore, once the thermistor is biased at some tempera-
ture above the ambient temperature of the fluid, the
additional power required to keep the thermistor at a
constant temperature when forced convection is present
(i.e. non-zero velocity) is a function of the velocity of
the fluid at the point of measurement.

3.2   Calibration of Probe

The measuring thermistor was biased at 4° C. above the
ambient temperature of the fluid, which was 37° C., using
the scheme shown in Figure 5.   (Detailed schematic diagrams
of the individual blocks are shown in Appendix 2.)   The
resistance of the thermistor at this level of heating (8 mw)
was about 1.2 Kohm.

The unheated reference thermistor T_R, shown in Figure 5,
did not provide adequate temperature compensation at this
stage, so the syringe driver and the probe were immersed in
a constant temperature bath which was maintained at 37° C.
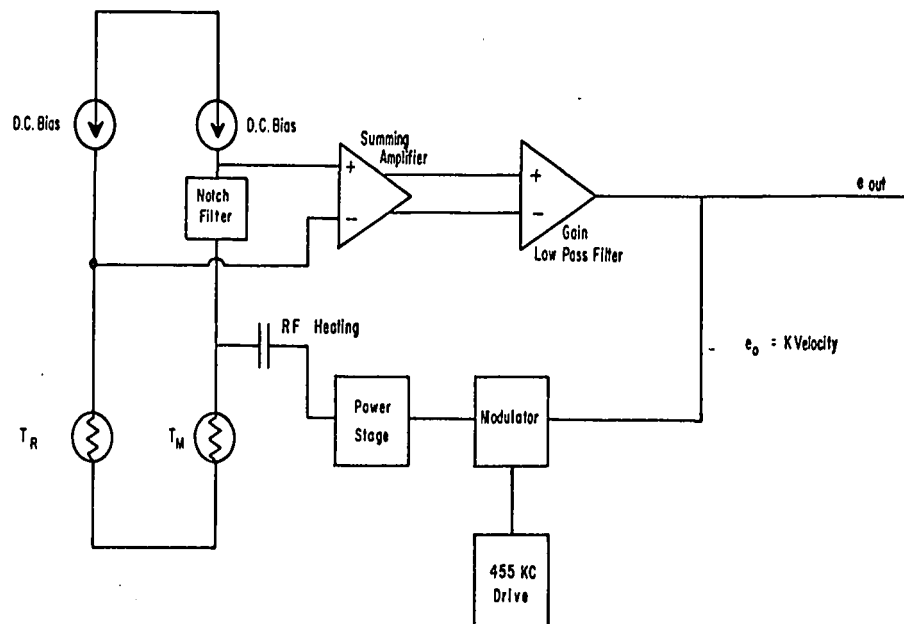
Figure 5. Initial flow meter scheme used for calibrations.

Using 0.16M saline as the fluid and a syringe driver to provide variable flow rates, the calibration curve shown in Figure 6 was obtained. Average velocities were calculated from the flow rates.

The slope of the curve shown in Figure 6 is ¼ (0.26). From this curve it is evident that the output voltage of the amplifier is directly proportional to the fourth root of velocity. This rapidly saturating non-linearity can, of course, be broken down into two square root functions in series. From the scheme shown in Figure 5 it is obvious that one square root non-linearity is due to the second power of current in Joule's Law. This is due to the fact

that the power fed into the thermistor is proportional to the square root of the output voltage of the system. The other square root non-linearity is then due to the non-linear forced convection heat transfer from the thermistor. This function does not agree with that obtained by Grahn, Paul and Wessel (1968, 1969). They reported that the heat transfer is a function of the log of velocity.
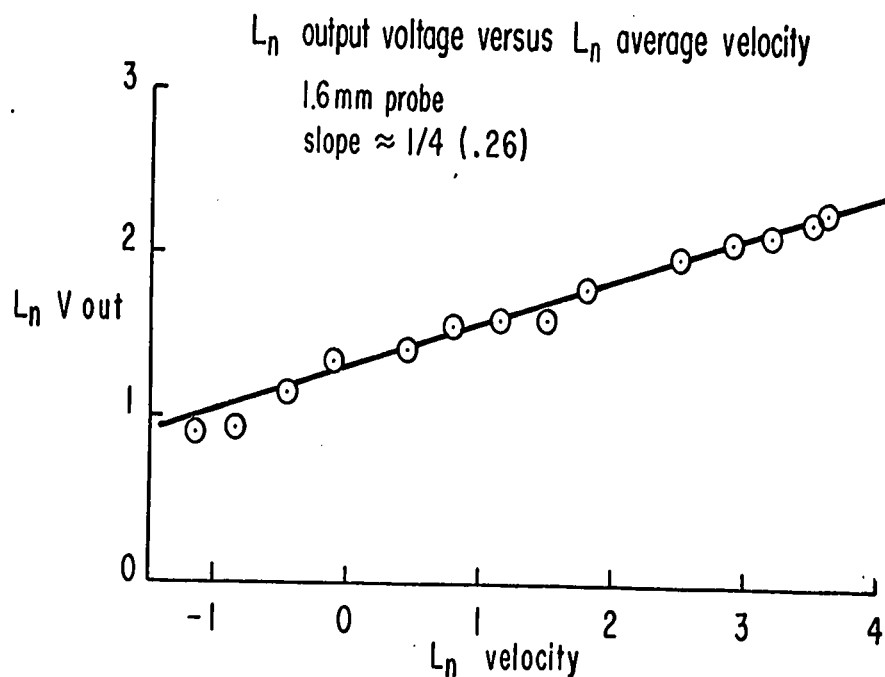
Figure 6. Calibration curve for 1.6 mm. diameter probe. The natural log of output voltage is plotted against the natural log of average velocity.

The system shown in Figure 5 is a regulator (input is zero). Therefore the square root function, due to Joule's

Law, in the forward path may be cancelled by insertion of

a similar non-linearity in the feedback path. This modifi-

cation is shown in Figure 8. A square root function was

generated using a diode network and an operational amplifier.

Another operational amplifier was used to eliminate sign

inversion and provide the offset for the bias power to the

measuring thermistor. The gain of the second amplifier was

set at ½ to allow the non-linearity to operate over a 10

volt range.
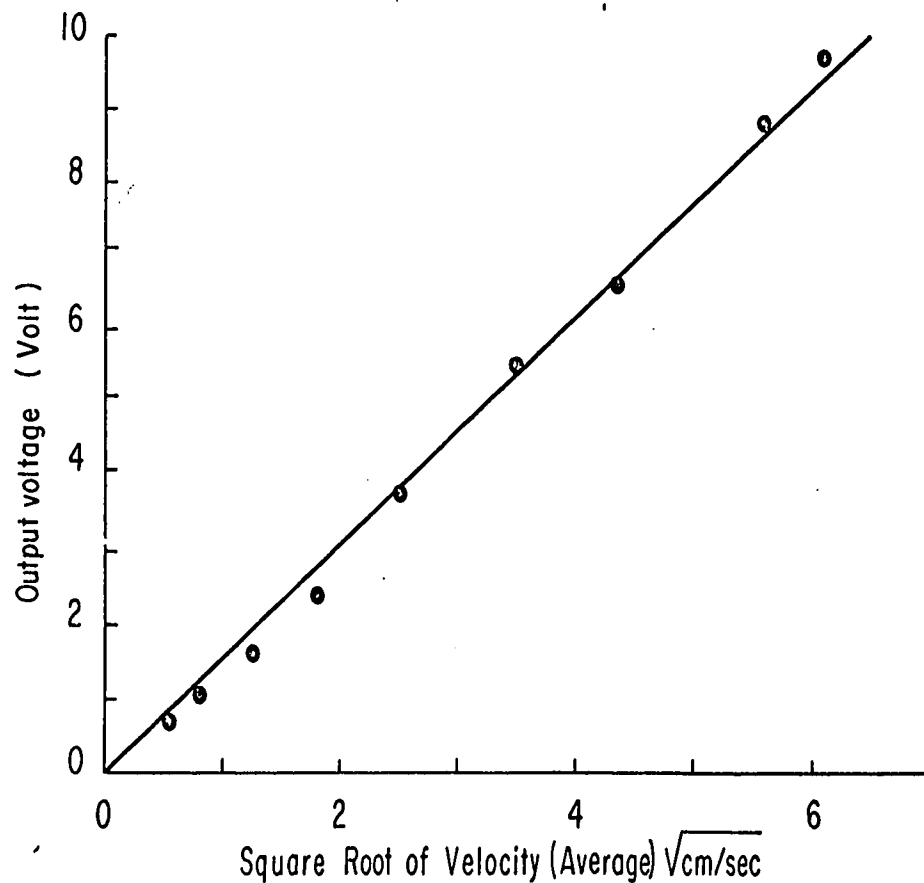
Figure 7. Calibration curve of 1.6 mm. diameter probe.

The flow meter scheme is the same as shown in Figure 5

except that a square root non-linearity has been inserted

in the feedback path. The output voltage is plotted versus

the square root of velocity.

A detailed schematic of the square root scheme is shown in Figures A-10 and A-11.
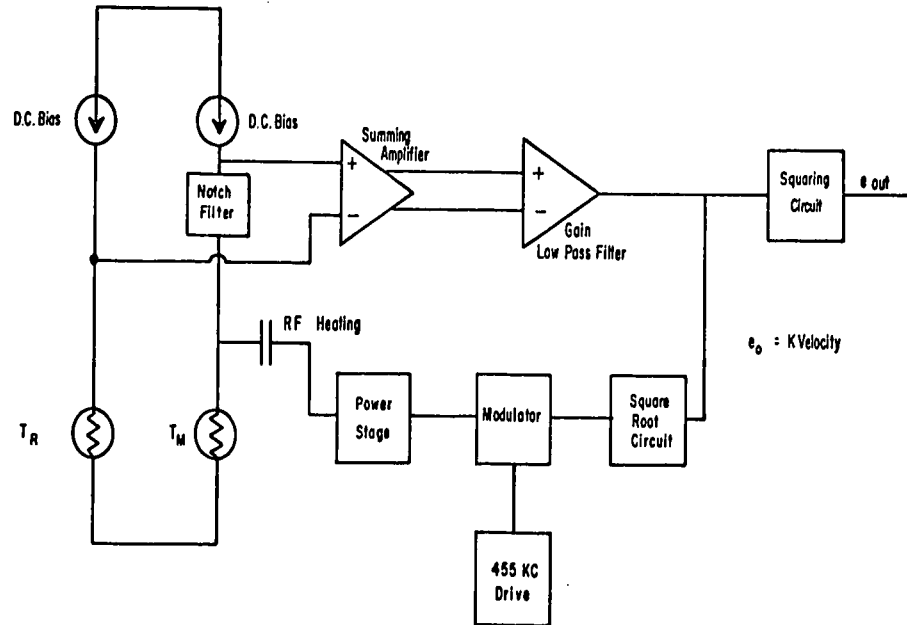
Figure 8. Complete scheme of the forced convection flow meter.

The additional modification was inserted into the scheme, as is shown in Figure 8, and a second calibration was performed using the same procedure as before. This was done in order to check the calibration deduced previously. A calibration curve is shown in Figure 7. The output voltage is now directly proportional to power.

The amount of heat transferred from the thermistor is

a function of the square root of velocity as is shown in
Figure 8. Since it was essential that the output voltage
of the flow meter be proportional to velocity, further
linearization was required. This linearization was easily
obtained by inserting a function which squares the output
voltage. The squaring function was generated using a diode
network and an operational amplifier. This function gener-
ator was preceded by a variable gain amplifier which
amplified the output signal as required so that at low flow
rates the entire 10 volt range of the non-linearity was
utilized (Figures A-12 and A-13).
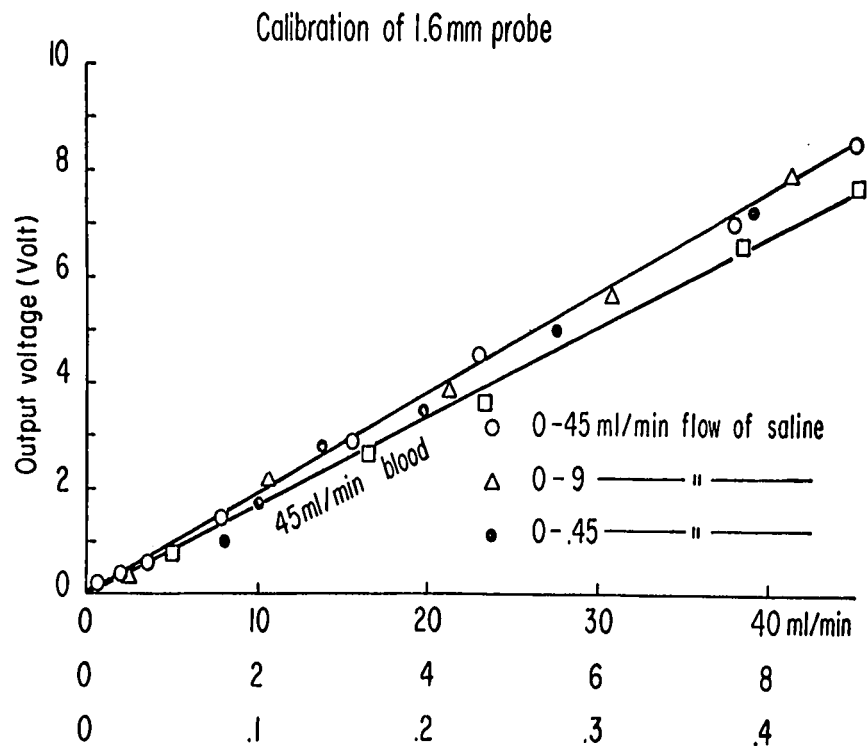
Figure 9. Calibration curves for the forced convection flow
meter. Whole dog blood or 0.16M saline was used as fluid.

The complete scheme of the forced convection flow
meter is shown in Figure 8. Calibration curves were
obtained for the flow meter using 0.16M saline and whole
dog blood. These curves are shown in Figure 9.

3.3 Theoretical Calculation of Heat Transfer

It has been stated before that the output of the
controlling amplifier which is a measure of the power
required to keep the temperature of the thermistor constant
is also a function of velocity. In steady uniform iso-
thermal flows the rate of convection heat loss from a solid
body depends not only on the flow velocity and body geo-
metry, but also on the physical properties of the fluid and
the difference in temperature between the fluid and the
solid body.

King (1914) derived a law relating heat transfer and
velocity in small cylinders. This law is an extension of
Boussinesq's (1905) earlier work and has been widely applied
to hot wire anemometry. King's Law is derived assuming
potential flow (viscosity = 0) which is a good approximation
for air flow. However, when considering flow of a viscous
fluid such as blood or 0.16M saline, potential flow is not
a good approximation. When the viscosity of a fluid is
non-zero, a fluid layer adjacent to a wall adheres to it.
The relative velocity between the layer of fluid and the
wall is zero. This type of flow is called boundary layer
flow where the boundary layer thickness is defined as the

distance from the wall to where the velocity approaches 99% of the free stream velocity.

Before an attempt was made to calculate the heat loss from the thermistor, some simplifying assumptions were made. They are as follows:

(1) The heat loss is calculated on the basis that the thermistor is spherical in shape.

(2) The heat loss from the platinum wires is small and thus neglected.

(3) The RF power goes into the thermistor and none is dissipated by the blood which is an ionic fluid (possible error eliminated by measurement).

(4) The effect of radiation to the fluid is small and may be neglected since temperature differences are small.

(5) The coefficient of heat conduction of the thermistor of radius r_o is very large compared with that of the surrounding medium so that the temperature of the sphere may be taken as uniform.

(6) The thermistor does not distort the flow field.

The equation of heat transfer (Landau and Lefshitz, 1959) in an incompressible fluid is as follows:

$$\frac{\partial T}{\partial t} + V \text{ grad } T = \frac{\kappa}{\rho C_p} \nabla^2 T \qquad \qquad ...(3.1)$$

where T = the temperature field

t = the time

V = the free stream velocity of the fluid

κ = the thermal conductivity of the fluid

C_p = the specific heat of the fluid and

ρ = the density of the fluid.

This equation neglects the temperature variation of κ, C_p and ρ which is valid since the temperature difference between the thermistor and the fluid is small. In calculating the heat transfer as a function of velocity, only steady convective flow is important and all time derivatives can be set to zero. It follows that

$$V \, grad \, T = \frac{\kappa}{\rho C_p} \, \nabla^2 T. \qquad \qquad ...(3.2)$$

In spherical co-ordinates, equation (3.2) becomes:

$$V_r \frac{\partial T}{\partial r} + \frac{V_\theta}{r} \frac{\partial T}{\partial \theta} = \qquad \qquad ...(3.3)$$

$$\frac{\kappa}{\rho C_p} \left(\frac{1}{r^2} \frac{\partial}{\partial r} \left(r^2 \frac{\partial T}{\partial r} \right) + \frac{1}{r^2 \sin \theta} \frac{\partial}{\partial \theta} \left(\sin \theta \frac{\partial T}{\partial \theta} \right) \right).$$

For flow around a sphere a two dimensional description of both temperature and velocity fields is sufficient since

$$\frac{\partial T}{\partial \phi} = \frac{\partial^2 T}{\partial \phi^2} = 0.$$

The θ and r components of velocity at low velocities (boundary layer flow) are

$$V_r = V \left(1 - \frac{3}{2} \frac{r_o}{r} + \frac{1}{2} \left(\frac{r_o}{r} \right)^3 \right) \cos \theta \qquad \qquad ...(3.4)$$

$$V_\theta = -V \left(1 - \frac{3}{4}\frac{r_o}{r} - \frac{1}{4}\left(\frac{r_o}{r}\right)^3\right) \sin\theta \qquad \ldots (3.5)$$

where r_o = the redius of the sphere and

  V = the free stream velocity.

Substitution of (3.4) and (3.5) into (3.3) results in a partial differential equation that is very difficult to solve. Numerical or successive approximation techniques are the only methods which will yield any type of solution.

Kudryashev and Smirnov (1965), using a simplified version of equation (3.3), obtained an approximate solution in closed form. Their solution for the heat transfer from a sphere (held at a constant temperature) due to forced convection is

$$Nu = 0.43 \sqrt{Re} \sqrt{Pr} \qquad \ldots (3.6)$$

where Nu = the Nusselt number

  Re = the Reynolds number and

  Pr = the Prandtl number.

$$Nu = \frac{P2r_o}{\kappa \Delta T} \qquad \ldots (3.7)$$

$$Re = \frac{V2r_o}{\nu} \qquad \ldots (3.8)$$

$$Pr = \frac{\nu \rho C_p}{\kappa} \qquad \ldots (3.9)$$

where P = the power dissipation per unit area in milliwatts per cm^2 and

  ν = the kinematic viscosity.

When the temperature difference and body geometry of the thermistor is taken into account, equation (3.6) may be

written as:

$$P_T = 0.74 \sqrt{V} \qquad \qquad \dots(3.10)$$

where P_T = the total heat transferred in milliwatts.

The approximate solution obtained by Kudryashev and Smirnov (1965) is plotted in Figure 10. The plot in Figure 10 is for a temperature difference of 4° C. Also shown in Figure 10 is the calibration curve (best fit straight line) from Figure 7 plotted as a comparison. Considering the assumptions which are involved in deriving the differential equation and solving it, the two curves agree reasonably well.
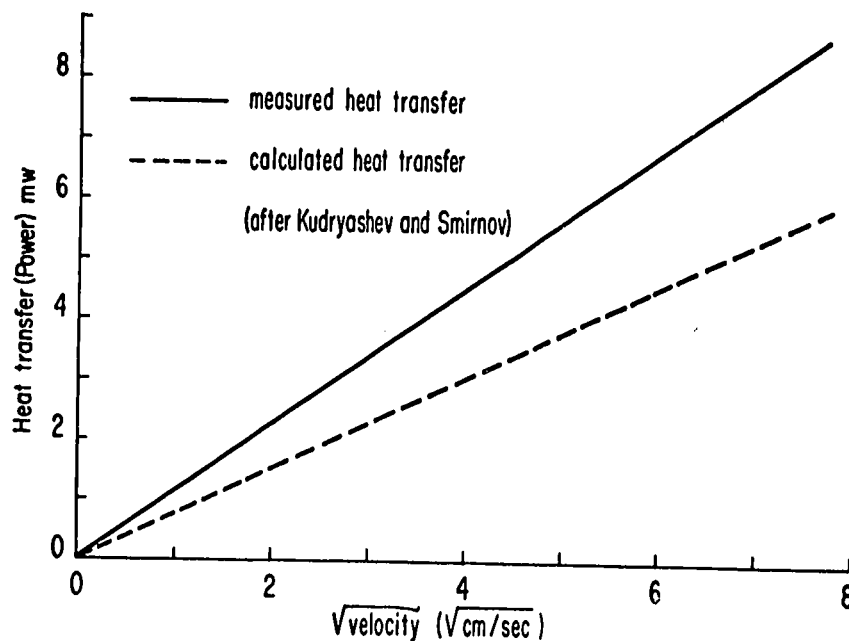
Figure 10. Comparison of theoretically calculated heat transfer from a constant temperature thermistor to the measured heat transfer.

The average velocity used in Figure 7 was corrected for a parabolic velocity profile before being plotted in Figure 10. The average velocity of a fluid calculated from the flow rate in a tube is ½ that of the maximum velocity at the center of the tube. The velocity at the thermistor was about 90% of the maximum velocity since the measuring thermistor was staggered off center as is shown in Figure 3.

The difference in the two curves shown in Figure 10 is probably due to several factors. They are:

(1) error in the temperature difference

(2) error in the dimension of the thermistor

(3) dissipation of a portion of the power in the fluid

(4) simplified form of the differential equation used in obtaining the theoretical curve (Kudryashev and Smirnov).

However the curves in Figure 10 indicate that the calibrations obtained by Grahn, Paul and Wessel are in error. This follows from the fact that their system gain is less than unity and hence the thermistor is not operating in the constant temperature mode. Rasmussen (1962) obtained a calibration curve for a thermistor operated in the constant current mode. His results agree with the results obtained by Grahn, Paul and Wessel. Both sets of results exhibit a logarithmic relationship between heat transfer and velocity. Figure 11 shows the measured heat transfer

due to forced convection obtained in this work. This is

compared with the heat transfer due to forced convection

reported by Grahn, Paul and Wessel (1968).
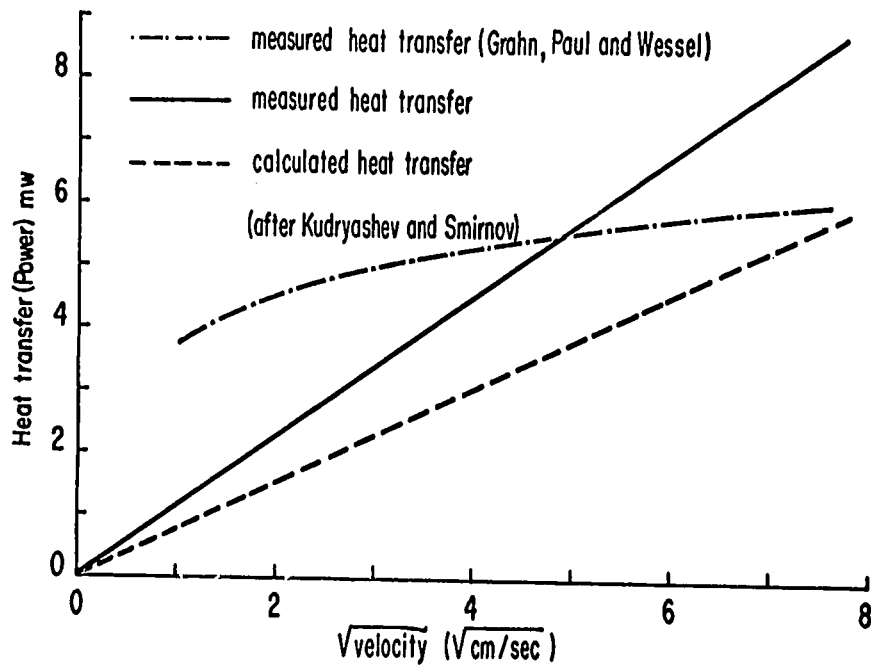
Figure 11. A comparison of the calibration curve obtained

in this work to the calibration curve reported (adjusted

for similar conditions) by Grahn, Paul and Wessel (1968).

Heat transfer is plotted versus the square root of velocity.

Also shown is the theoretical curve calculated from the

equation (3.10).

The curve obtained by Grahn, Paul and Wessel was

corrected before it was plotted in Figure 11. Adjustment

of their results was required because the temperature

difference used in their calibration was 13° C. and the

dissipation constants of the thermistor used in their work
was 40% less than that of the thermistor used in this work.
Also shown in Figure 11 is the calculated result using the
equation derived by Kudryashev and Smirnov (1965).

3.4 Temperature Compensation

The reference thermistor is biased with about ½ the
value of the D.C. bias used for the measuring thermistor.
It receives no RF heating. Because of the very low power
dissipation the reference thermistor is relatively insen-
sitive to velocity (James, Paul and Wessel, 1966). This
insensitivity to velocity follows from equation (3.10).
When the temperature difference is zero there can be no
heat transfer. The D.C. bias through the reference ther-
mistor can be varied using a 10 turn potentiometer which
varies the supply voltage to the current source. The
current source is a resistance of 82 Kohm. The variation
in current to the reference thermistor is used to provide
a balance for zero velocity in the probe. Thermistor
characteristics vary with time (aging) and thus this
balance must be checked periodically.

Since the measuring thermistor is heated with 8 mw
of power and the reference thermistor is unheated, the
temperature coefficients of resistance differ in the two
thermistors. Therefore, as the temperature of the fluid
changes, the reference thermistor will not provide a
proper reference signal.

A parallel resistor across the measuring thermistor
was used to compensate for differences in temperature
sensitivity α, where α is derived from equation (2.1)
and

$$\alpha = \frac{1}{R} \left(\frac{dR}{dT}\right) = -\beta \frac{1}{T^2} . \qquad \qquad ...(3.11)$$

This parallel resistor was picked by trial and error.
Figure 12 shows the error in zero balance of the flow
meter due to temperature deviations from 37° C. The
temperature tracking of the two thermistors is good over
a temperature range of 4°. A 10 mV offset would be equal
to an error which is 10% of full scale on the most sensitive
flow range (0.45 cc./min.). Periodic checks of the temper-
ature compensation scheme indicate that α is relatively
insensitive to aging.

Figure 12 shows that the compensation is valid for a
small temperature range. The error becomes greater as the
temperature is greatly changed from the balance condition
at 37° C.

Another possible source of error in velocity measure-
ments was due to the actual change in resistance of the
measuring thermistor due to temperature. This changes the
temperature difference between heated thermistor and fluid.
For example, if the temperature increases, the resistance
of the thermistor decreases, but the power dissipated
increases. However, over a small temperature range of up
to 2 degrees, the error would be in the order of 2% of
full scale flow (0.45 cc./mm.).
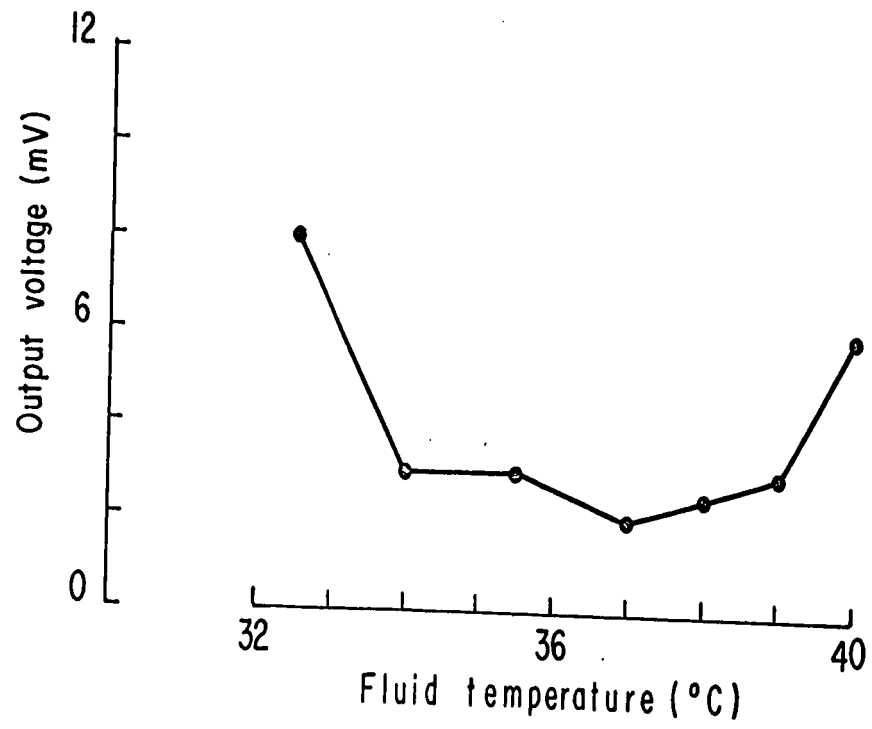
Figure 12. Error in zero balance versus temperature
deviations from 37° C. Zero offset is plotted as output
voltage.

4.1 Time Constant of the Thermistor

The resistance of a thermistor as a function of absolute temperature is given by equation (2.1). When a thermistor is heated to a temperature T, and permitted to cool, the rate of cooling is found to be proportional to the instantaneous temperature difference $T - T_x$, T_x being the temperature of the surrounding fluid. The heat transfer equation is therefore:

$$C \frac{dT}{dt} = K(T - T_x) \qquad \qquad \ldots (4.1)$$

where C = the heat capacity and

K = the dissipation factor.

The time constant is defined as:

$$\tau_1 = \frac{C}{K} . \qquad \qquad \ldots (4.2)$$

Equations (4.1) and (4.2) apply to either an indirectly heated thermistor or to one in which the dissipation of power is small so as to produce negligible heating. A more general heat transfer equation is:

$$C \frac{dT}{dt} = P - K(v) (T - T_x) \qquad \qquad \ldots (4.3)$$

where P = the power dissipated in the thermistor.

In general, $K(v)$ depends on the thermodynamical properties of the fluid and the speed of the fluid relative to the thermistor. The time constant of a thermistor is reduced as a consequence of power dissipation in the thermistor and

the velocity of the surrounding fluid.

Rasmussen (1962) has shown that the time constant of a self-heated thermistor in a fluid is given by:

$$\tau_2 = \frac{C}{K(v) - P_o \alpha} \qquad \ldots(4.4)$$

where P_o = the initial power specified at t = 0 and

$$\alpha = \frac{-\beta}{T^2} .$$

This agrees with the equation derived by Janssen, Ensing and Van Erp (1959) for a hot wire.

From equations (4.2) and (3.11) the new time constant for a heated thermistor in a fluid stream is given by the expression:

$$\tau_2 = \frac{\tau_1}{(1 + \frac{\beta P_o}{T_o^2 \, K(v)})} \qquad \ldots(4.5)$$

where β = a constant which depends on the material used to make the thermistor.

The function K(v) is a function of velocity. In Chapter 3 it was shown by measurement that:

$$K(v) = 2 + 0.225 \sqrt{v} \text{ mw./degree} \qquad \ldots(4.6)$$

where 2 mw./degree is the amount of power required to provide the initial bias of temperature difference between the thermistor and the fluid. Figure 13 is a signal flow diagram of the forced convection flow meter without the output squaring circuit.
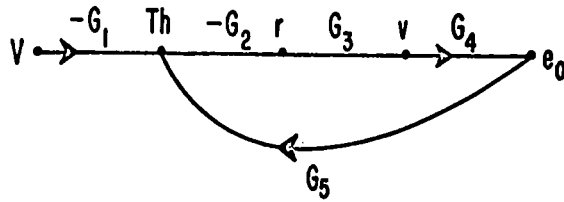
Figure 13. Signal flow diagram of forced convection flow meter.

The transfer functions (using Laplace transformation) in Figure 13 are:

$$G_1 = \frac{0.9}{\sqrt{V}} \qquad \ldots (4.7)$$

$$G_2 = \frac{K_1}{1 + s\tau_2} \qquad \ldots (4.8)$$

$$G_3 = K_2 = 0.1 \times 10^{-3} \qquad \ldots (4.9)$$

$$G_4 = K_3 = \frac{1 \times 10^4}{(1 + s\tau_3)(1 + s\tau_4)} \qquad \ldots (4.10)$$

$$\tau_2 \gg \tau_3, \tau_4$$

$$G_5 = K_4 \qquad \ldots (4.11)$$

The static loop gain K, is equal to $K_1 \times K_2 \times K_3 \times K_4$ and was measured to be 2.1×10^3. The transfer function, assuming τ_3 and $\tau_4 = 0$, can be written as:

$$\frac{e_0}{V} = \frac{G_1}{G_5} \frac{K}{K + 1} \frac{1}{1 + s\tau_8} \simeq \frac{G_1}{G_5} \frac{1}{1 + s\tau_8} \qquad \ldots (4.12)$$

where $\tau_8 = \frac{\tau_2}{K + 1}$.

Equations (4.11) and (4.12) show that the effective time

constant at zero velocity of the thermistor has been
decreased by a factor equal to approximately 1/K. The
time constants τ_3 and τ_4 were set to further filter the
RF heating voltage. They were incorporated into the
summing amplifier.

4.2 Bandwidth of System

The static loop gain K, for the system was measured
to be 2.1×10^3. The effective time constant of the
thermistor in air is about 0.25 msec. The corner frequency
measured using an air pulse, was estimated to be 600 Hz
which corresponds well to the calculated value. Attempts
to further increase the bandwidth by increasing the system
gain was made impossible by instability, indicating that
at least another time constant exists. The bandwidth in
air could be further extended by inserting a lag network
in the feedback path. This has the same effect as a lead
network in the forward path. In this way the bandwidth
could be further increased to 0.9 KHz before instability
occurred. Figure 14 shows the response of the flow meter
to a step function of air with a rise time of about 0.22
msec. The limiting time constant in this case is the two
output filters (corner frequencies 190 Hz and 160 Hz).
The bandwidth of the flow meter with saline (or blood)
as the fluid is at least as high as that in air since the
effective time constant of the thermistor in saline is
less than that in air (equation 4.2).

2 msec
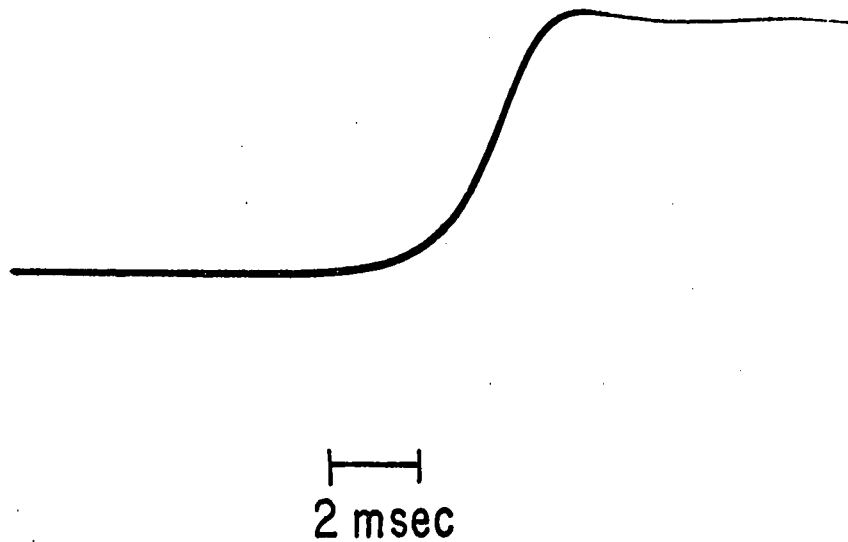
Figure 14. Response of flow meter to step of air flow.
(limited by two output filters.) The flow meter was not
calibrated for air velocity.

In order to get an approximate idea of the bandwidth
of the flow meter with 0.16M saline as the fluid, a small
resistor ($\frac{1}{4}$ ohm) was placed in series with the measuring
thermistor. Initially this resistor was shorted. When
the short was removed the effective resistance of the
measuring thermistor was increased. The system responded
with an instantaneous increase in power which came back
to balance as the thermistor heated up. The system
returned to balance exponentially from which the time
constant was estimated. The optimal response of the system
was set using the compensating network in the feedback
path. The response varied from oscillatory to over-
damped.

The transfer function of the compensating network is (Figure A-10):

$$G_5 = \frac{K_4 \ (s\tau_5 + 1)}{(s\tau_5 + 1) \ (s\tau_6 + 1) + s\tau_7} \cdot \qquad \ldots(4.13)$$

The optimal bandwidth was estimated to be about 1.2 KHz. Figure 15 shows the response of the flow meter to a ¼ ohm increase of thermistor resistance with 0.16M saline at zero velocity in the probe. Since this is a much higher bandwidth than required, two first order filters were placed at the output in order to limit the bandwidth at about 125 Hz.
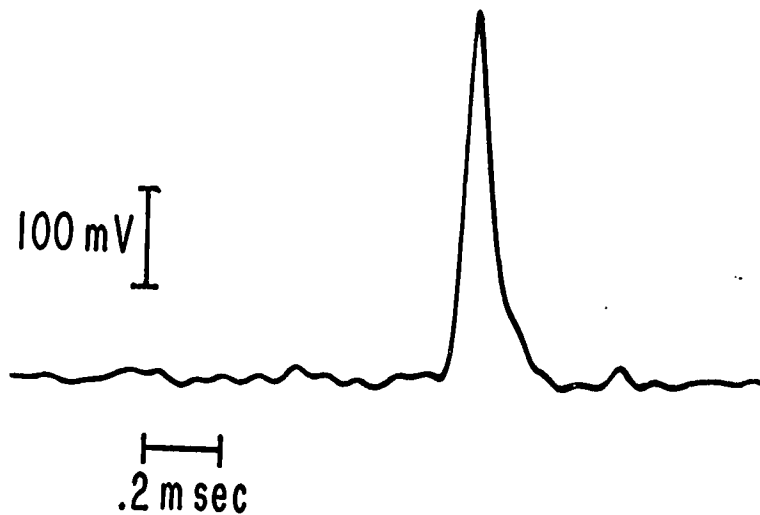
Figure 15. Response of system to a ¼ ohm change of resistance in series with the thermistor.

Figure 15 shows the response actually depends on two time constants. One is the speeded up time constant of the system τ_8. The second is slower. It is due to the heat capacity of a layer of fluid next to the thermistor and is also dependent on the velocity of the fluid, since the thickness of the boundary layer decreases with increased velocity.

$$\delta \propto \frac{1}{\sqrt{Re}} \qquad \qquad ...(4.14)$$

where δ is the boundary layer thickness. This second time constant limits the maximum bandwidth of the system where a fluid such as water or saline is involved. In air it exists but it is much smaller than in saline.

An equation (Corrsin, 1963) which approximates the value of the second time constant is:

$$\tau_9 = \frac{d^2}{D} \qquad \qquad ...(4.15)$$

where d = a function of geometry of the thermistor and

the velocity of the fluid and

D = the thermal diffusivity of the fluid.

At zero velocity the value of $\tau_9 \approx 0.2$ seconds, while $\tau_2 \approx 0.02$ seconds, so that the limiting bandwidth is set by the slower time constant. If only τ_2 was present, the maximum bandwidth at zero velocity would be in the order of 15 KHz.

The two time constants are a function of velocity and as a result, the flow meter responds faster to increasing velocities than to decreasing velocities. In part, this is

due to the effect of velocity on frequency response. More important is the fact that the requirement for an increase in thermistor heating with increasing velocity can be met electrically by increasing the heating power. On the other hand, the required cooling of the thermistor cannot be accomplished simply by decreasing the heating power. In addition to a decrease in heating power, cooling requires heat dissipation.

4.3 Stability of the System

The system with a static loop gain of 2.1×10^3 was stable. Instability did not occur until the gain was increased to about 2.5×10^3. The system with the square root non-linearity in the feedback path behaves as a linear system. However the heat transfer due to forced convection which is the input is a non-linear function of velocity. The characteristic equation of the system determines its stability. It is:

$$1 + G(s) \ H(s) = 0 \qquad \qquad ...(4.16)$$

where $G(s)$ = the transfer function of the forward path

and $H(s)$ = the transfer function of the feedback path.

The system with the compensating network in the feedback path should theoretically be stable for all values of gain. This is true even if the second (postulated) time constant is included. However at very high values of gain, the time constants which were set to filter out the RF power will cause instability. These time constants are τ_3 and τ_4.

Other time constants exist but they are smaller than τ_3 and τ_4.

The root locus diagram is a method of showing the degree of stability achieved. It is a plot in the s-plane of the roots of the characteristic equation of the closed loop system as a function of gain. The underlying principle of this method is based upon the fact that closed loop poles are related to poles and zeros of the open loop transfer function G(s) H(s) and to the gain. The roots of the denominator of G(s) H(s) are called poles and roots of the numerator are called zeros when all the coefficients of s are equal to unity.

The characteristic equation of the system, including the second time constant and the compensating network, is given by:

$$1 + \frac{500\ (s + 640)}{(s + 5)\ (s + 50)\ (s + 1500)} = 0 \qquad \ldots (4.17)$$

where (s = -5) and (s = -50) are the poles due to the thermistor and the fluid. The other pole and zero are due to the compensating network. The compensating network has another pole but it is very large compared to the other poles. A root locus diagram of the system is shown in Figure 16. Also shown in Figure 16 is the effect of another pole at $s = -80 \times 10^3$ which exists in the system. This one additional pole has the effect of driving the system into instability at higher values of gain. The system contains several such poles and hence this is one reason why the

system becomes unstable. An approximate value gain from the root locus diagram for which the system becomes unstable is 3.4×10^3 which is greater than the measured value of 2.5×10^3. This difference in the gains could be due to the effect of other poles at s very large. Several such poles would cause a decrease in the gain. Contribution of such poles would be small. The major reason for this difference is probably that a one time constant approximation is an over-simplification of the actual lag due to the fluid layer. However the root locus diagram does prove that it is a reasonable assumption.
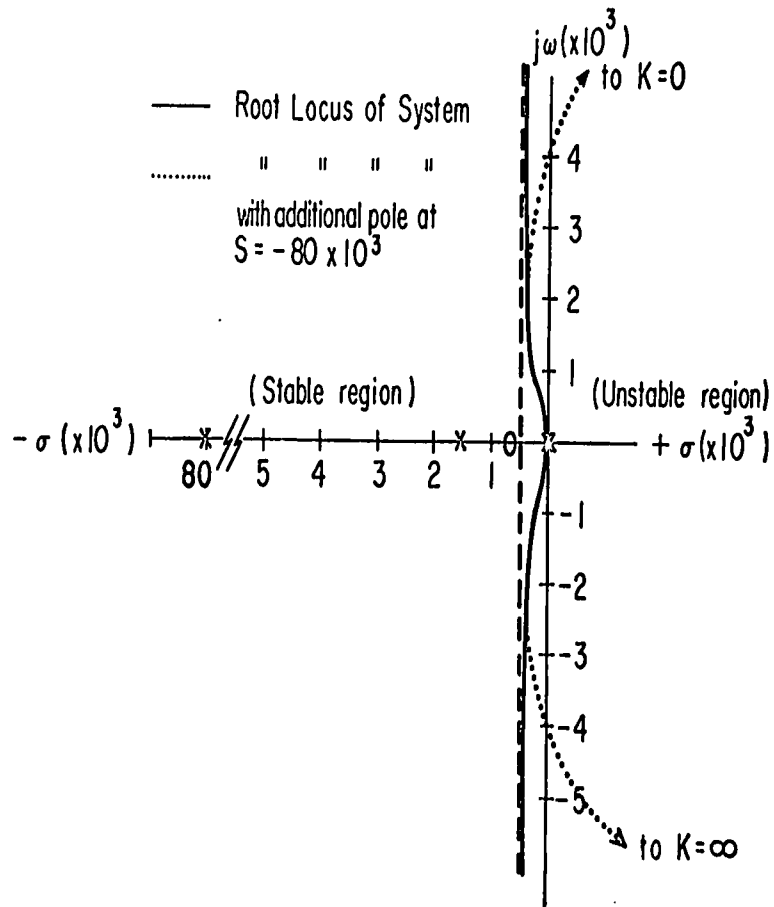
Figure 16. Root loci of the system. The effect on the root locus of a pole at s = -8 × 10^4 is also shown.

Chapter 5   CONTROL OF BLOOD FLOW TO THE

SUBMAXILLARY GLAND

5.1 Literature Review

Forced convection flow measurement techniques, because
of their sensitivity, are applicable to the measurement of
blood flow to glands. The control of blood flow to glands,
such as the submaxillary gland, has been a controversial
problem throughout the last century.

5.1A Blood Flow and Secretion

This problem dates back to the work of Claude Bernard
(1858), who presented evidence for the existence of vaso-
motor nerves (constrictor and dilator) in the submaxillary
gland. He showed that stimulation of the parasympathetic
nerve supply to the gland produced vasodilatation, whereas
sympathetic nerve stimulation produced vasoconstriction.
From this it was generally accepted that vasodilator and
vasoconstrictor autonomic nerve fibers ended in close
proximity to, and acted directly on, the blood vessels.
Later it was observed by Carlson (1907) that sympathetic
vasoconstriction was followed by vasodilatation.

Previous to the work of Claude Bernard, Ludwig (1851)
had shown that stimulation of the chorda tympani nerve or
of the cervical sympathetic chain resulted in secretion of
saliva from the submaxillary gland of the cat. The
observations by Ludwig were pursued by Heidenhain (1872)

who made the observation that atropine completely blocked the secretion produced by stimulation of the chorda tympani nerve while the vasodilatation was unaffected. Thus for many years it was generally accepted that there were separate secretory and vasomotor nerve fibers in both the parasympathetic and sympathetic nerves to the gland.

The first group to challenge the existence of vasodilator nerve fibers was Barcroft and his co-workers (Barcroft and Müller, 1912; Barcroft and Piper, 1912; Barcroft, 1914) who expressed the view that secretory metabolism in the submaxillary gland determined vasodilatation. Barcroft (1914) concluded (from experiments in which oxygen consumption was measured in the gland before and after atropine) that the increased blood flow was secondary to increased metabolic activity, since increased oxygen consumption, like vasodilatation, was unaffected by atropine. More detailed analysis of Barcroft's work by Bayliss (1923) revealed that the increased metabolic rate and increased vasodilatation produced by nerve stimulation after the administration of atropine were by no means closely correlated. Bayliss maintained that the vasodilatation was controlled by parasympathetic dilator nerve fibers.

Those workers who supported the theory that a relationship existed between blood flow and metabolism did not postulate any chemical mediator whereby the increased

metabolism produced vasodilatation. Werle and von Roden (1936) showed that the potent vasodilator substance, kallikrein, was present in the submaxillary gland and that its effects were atropine-resistant. This led immediately to the suggestion by Ungar and Parrot (1936) that kallikrein was the compound which mediated vasodilatation in the salivary gland when the chorda tympani nerve was stimulated.

For about twenty years little attention was paid to the contention of Ungar and Parrot. However, during the period from 1955 onwards Hilton and Lewis (Hilton, 1960, 1962, 1963; Hilton and Lewis, 1955a, b, 1956, 1957, 1958; Lewis, 1960, 1962, 1963) took up the problem and published a series of papers, not only maintaining the conclusion put forward by Ungar and Parrot, but also suggesting its extension to cover functional vasodilatation in organs generally. A significant generalization has developed from the conclusions of Hilton and Lewis: true parasympathetic vasodilator nerve fibers do not exist. Schachter and his co-workers (Beilenson, Schachter and Smaje, 1965, 1968; Bhoola, Morley, Schachter and Smaje, 1965; Morley, Schachter and Smaje, 1966; Schachter and Beilenson, 1967, 1968) have strongly challenged the conclusions of Hilton and Lewis on the basis of their work on the salivary glands of the cat, rabbit, sheep and dog.

The mechanism of parasympathetic induced vasodilatation in salivary glands, as indicated in the history, is in dispute. Basically, the two theories are:

(1) parasympathetic cholinergic vasodilator
nerve fibers exist, but for some reason
produce responses that are atropine-resistant,

(2) parasympathetic vasodilator nerve fibers do
not exist and the vasodilatation that is
produced upon parasympathetic nerve stimula-
tion is mediated by kallikrein which is
released from the secretory cells.

Hilton and Lewis, supporters of the second theory,
maintain that during secretory activity an enzyme, kalli-
krein, passed from the salivary gland secretory cells into
the interstitial fluid where it acts on an α_2-globulin
substrate to release a vasoactive peptide (kallidin). They
based their conclusions on the following experimental
evidence:

(1) The output of kallikrein in the venous out-
flow of a perfused cat submaxillary gland
increased greatly upon chorda tympani nerve
stimulation, even after atropine had been
injected close-arterially, although in the
latter case the increase was not quite as
great.

(2) When the chorda tympani nerve was stimulated
for the first fifteen seconds of a sixty
second arterial occlusion, dilatation
occurred when the occlusion was removed;

chorda stimulation during venous occlusion
also caused a post-occlusion vasodilata-
tion, but only if the lymph drainage had
been removed.

These results were interpreted by Hilton and Lewis
as indicating that a metabolic vasodilator material which
was normally removed by the lymph system, and which was
probably a bradykinin-releasing enzyme (kallikrein), was
the mediator of the vasodilatation induced by chorda
tympani nerve stimulation. Presumably if the mediator of
vasodilatation were acetylcholine, it would have been
destroyed during the period of arterial occlusion.

The theory put forward by Hilton and Lewis has been
most strongly challenged by Schachter and his co-workers.
Bhoola, Morley, Schachter and Smaje (1965) challenged the
theory put forward by Hilton and Lewis on the following
evidence:

(1) Close-arterial injection of saliva into a
gland with natural circulation failed to
duplicate the vasodilatation produced by
stimulation of the chorda tympani nerve.
The changes in blood flow were slower in
onset and were never as large as those pro-
duced by nerve stimulation or injection of
bradykinin or acetycholine. The changes
produced by saliva were more prolonged.

(2) After desensitization of the blood vessels
to a standard dose of bradykinin, it was
found that the response to chorda tympani
stimulation or acetylcholine injection was
reduced to a lesser degree.

(3) It was possible to produce a maximal
atropine-resistant vasodilatation by stim-
ulation of the chorda tympani nerve when
the gland had been perfused by horse serum
for as long as three hours. (It had been
shown previously that cat saliva fails to
release kinin from horse serum.) Under
these conditions close arterial injections
of dialysed saliva failed to cause vasodila-
tation.

Beilenson, Schachter and Smaje (1968) found that it
was possible to deplete the cat submaxillary gland of
kallikrein by chronic ligation of the duct, and by sympath-
etic stimulation. In such cases, the amount of kallikrein
remaining was 0.1% of the control. Such glands nevertheless
responded to chorda stimulation with a normal atropine-
resistant vasodilatation. Also, they reported that
sympathetic nerve stimulation produced saliva with a higher
concentration of kallikrein than parasympathetic nerve
stimulation.

Several other groups of workers have presented evidence

which challenges the theory that kallikrein plays a role in parasympathetic vasodilatation. Degeneration studies by Kuntz and Richins (1946) showed that extirpation of the superior cervical ganglion resulted in the expected decrease in the number of fibers related to blood vessels; however, considerable innervation still remained.

Snell and Garrett (1958), using histochemical and degeneration techniques, showed that fibers from the chorda tympani nerve supplied branches to ducts and arteries. Electron microscope work by Garrett (1966c, d) on the submaxillary gland of the cat showed that the blood vessels receive a dual parasympathetic and sympathetic innervation.

Terroux, Sekelj and Burgen (1959) showed that moderate doses of atropine depressed salivation as well as the accompanying increase in oxygen consumption without affecting the chorda tympani induced vasodilator response in the dog submaxillary gland. This seems to indicate that the metabolic and vasodilator effects of parasympathetic nerve stimulation may be separated.

Strömblad and Dresel (1963) reported that injection of hemicholinium (HC-3) into the duct of the parotid gland of the cat gradually blocked parasympathetic induced vasodilatation. Hemicholinium gradually decreases the release of acetylcholine by diminishing the resynthesis of acetylcholine in nerve fibers. Work by Prasad and Mac Leod (1966) suggests that HC-3 may also alter the sensitivity of the smooth muscle receptors to acetylcholine. These results

support the theory that acetylcholine mediates a signifi-
cant portion of parasympathetic induced vasodilatation in
cat salivary glands; however, they do not eliminate the
possibility that acetylcholine only mediates an inter-
mediate step.

Skinner and Webster (1968) showed that the vasodilator
effects of chorda tympani stimulation were unaffected in
cats pre-treated with carboxypeptidase B (a potent inactiv-
ator of bradykinin or kallidin), whereas the equivalent
vasodilator effects of kallidin injected close-arterially
were abolished. They suggest that the major part of chorda
vasodilatation is due to the presence of adrenergic neurones
in the chorda tympani nerve which cause vasodilatation via
β-adrenergic receptors which are present in the blood
vessels. They also report that parasympathetic vasodilata-
tion is suppressed by propranolol (a β-receptor-blocking
drug) and that propranolol blocks the vasodilatation
produced by isoprenaline injected close-arterially.

These results are challenged by Schachter and Beilenson
(1968), who have confirmed the observations of Skinner and
Webster (1968) with propranolol, but have also reported a
decreased sensitivity to acetylcholine with increased doses
of propranolol. Reserpine, which depletes noradrenalin,
has been used in cats by Davey, Davies, Reinart and
Scholfield (1965), and those authors report that parasym-
pathetic stimulation is unchanged while sympathetic effects
are abolished. These results were confirmed by Schachter

and Beilenson (1968).

In 1967 Hilton and Torres repeated the work by Beilenson, Schachter and Smaje (1965) and reported that the kallikrein content drops to only three percent of the control value, and that in such glands there was an increased sensitivity to bradykinin and that the sensitivity to close-arterial injections of acetylcholine was the same as that in normal glands. After further depletion of the glandular kallikrein by stimulation of the sympathetic nerve, Hilton and Torres (1967) reported that the parasympathetic vasodilator response was then reduced.

Hilton (1970) maintains that parasympathetic vasodilatation is mediated by kallikrein and that parasympathetic vasodilator nerves do not exist; on the other hand, Schachter and his co-workers suggest that kallikrein plays no role in parasympathetic vasodilatation. Schachter and his co-workers also suggest that parasympathetic vasodilatation is cholinergic, but is in some way resistant to atropine.

Hilton and Lewis (1956) have extended their theory of kallikrein-kinin mediated parasympathetic vasodilatation to cover the vasodilatation which occurs on cessation of sympathetic nerve stimulation. Meanwhile, Bhoola, Schachter and Smaje (1965) have suggested that the after-dilatation is due to activation of β-adrenergic receptors in the arterioles, and that the kallikrein-kinin system probably

plays no role.

5.1B Electrophysiology

Recent electrophysiological work by Creed and Wilson (1969) on the response of secretory acinar cells to nerve stimulation in the submaxillary gland of the cat suggest further experiments which may help resolve the controversy. Bayliss and Bradford (1886) discovered that during secretion an electrical potential could be measured between the hilus and the surface of the gland. They found that the electrical change (electrogram) was abolished by atropine. Bradford (1887) showed that the flow of saliva did not cause the electrogram since compression of Wharton's duct did not affect the electrogram. Moreover, the outflow of saliva after removal of the obstruction did not produce the electrogram. He concluded that the electrogram originated from the glandular cells and that it preceded secretion of saliva.

Further electrophysiological work on the cat submaxillary and sublingual glands was reported by Lundberg (1955, 1957a, b, c, 1958). He used intracellular recording techniques to measure electrical changes in secretory cells of the submaxillary gland and reported a resting potential of -15 to -30 mV. Lundberg (1955) reported that stimulation of either the sympathetic or parasympathetic nerve supply to the gland produced a hyperpolarization, i.e. a secretory potential, across the outer membrane of individual acinar

cells. These hyperpolarizations occurred after a latency period of 0.6 to 1.0 sec. for sympathetic, and 0.2 to 0.4 sec. for parasympathetic nerve stimulation. Lundberg (1955) concluded that a relationship existed between secretory potentials and secretion since, in cases where there was a diminished secretion from a gland after a period of anoxia, or after atropine, the secretory potentials decreased in parallel to secretion. Since Lundberg (1955) was able to show an increase in membrane potential with an increase in strength of single stimuli to the chorda tympani nerve (multiple fiber summation), he suggested that five to ten parasympathetic neurons supplied each secretory cell.

The typical response obtained from the secretory cells was named the type 1 response by Lundberg (1955). He also recorded responses from two other types of cells. The type 2 response had a resting potential of 35 mV. The response to parasympathetic nerve stimulation was a hyperpolarization after a latency of 400 msec. while the response to sympathetic nerve stimulation was a depolarization. Lundberg suggested that the type 2 response originated from the demilune cells. The type 3 response which originated from the duct cells responded to both parasympathetic and sympathetic nerve stimulation with a depolarization after a latency of several seconds.

Garrett (1966c, d) described small extra-acinar

bundles of nerve fibers in close relationship to secretory cells with the smallest distance between a nerve bundle and acinus being 1000 Å. Garrett further suggested that neuro-effector sites might occur where the axons within these bundles become partly free of Schwann cell investments.

Creed and Wilson (1969) report that the hyperpolarization response to preganglionic parasympathetic nerve stimulation and to post-ganglionic sympathetic nerve stimulation was dependent on the frequency of stimulation. The mean latency of the hyperpolarization response to parasympathetic nerve stimulation at 1, 8 and 100 pulses per second was 273, 420 and 252 msec. respectively. The hyperpolarization response to sympathetic nerve stimulation did not occur until the frequency was over 5 pulses per second; the latency was over 420 msec.

Ultrastructure studies by Creed and Wilson (1969) revealed bundles of unmyelinated fibers between acini; some of the axons were free of Schwann cell investment and contained agranular and granular vesicles. Creed and Wilson also revealed that single nerve fibers were found in intra-acinar positions between the membrane of adjacent secretory cells and these axons contained agranular vesicles. The two membranes (axon and acinar cell) were about 160 Å apart. On the basis that the secretory cells respond to single stimuli of the parasympathetic nerves and only to

repetitive stimuli of sympathetic nerves, Creed and Wilson suggest that the nerves which are 160 Å away from the acinar cell are parasympathetic. Using Richardson's (1964) conclusion that cholinergic axons contain agranular vesicles and occasional larger vesicles with an electron dense central area, and that adrenergic nerve fibers contain both agranular vesicles and small vesicles with a dense core, the intra-acinar fibers are suggested by Creed and Wilson to be cholinergic while the extra-acinar nerves may be derived from both a cholinergic and an adrenergic supply.

The paper by Creed and Wilson suggests an experiment which could partially clarify the problem of the control of parasympathetic vasodilatation. If blood flow can be shown to increase within the latency of the hyperpolarization of the secretory cells, then the vasodilatation cannot be secondary to the secretion of saliva. The mechanism for the secondary action would be the release of kallikrein into the interstitial fluid and the subsequent release of kallidin with resulting vasodilatation. If the blood flow changes show a longer latency than hyperpolarization, the results would then not be very conclusive; although these latencies may be due to mechanical factors, such as transport delays within the gland and the time required to change the size of blood vessels due to smooth muscle relaxation. Transport delays within the gland could be due to the large increase in capacity of the gland caused by vasodilatation. Another latency could be due to the release and diffusion

of transmitter, although this would probably be short as has been suggested by Creed and Wilson (1969).

If the latency between nerve stimulation and an increase in blood flow (vasodilatation) is less than a second, it is unlikely that parasympathetic vasodilatation is mediated by an enzyme system such as kallikrein and bradykinin. Time course studies such as these would not be conclusive proof of the existence of parasympathetic vasodilator fibers unless accurate information on the enzyme kinetics involved was also available. However, bio-assay studies on the kallikrein-kinin system seem to indicate a slow system. More conclusive proof of the presence of parasympathetic vasodilator fibers could be provided if electrophysiological events in the smooth muscle cells in the walls of blood vessels could be correlated to parasympathetic and sympathetic nerve activity. The latency of the electrical response of the vascular smooth muscle may well give a final answer to the question of whether parasympathetic vasodilator nerve fibers do exist or not in the submaxillary gland.

5.2 Objectives of Present Work

The first objective was to use electrophysiological techniques to measure the membrane potential changes of secretory cells as has been reported by Creed and Wilson (1970) and, if possible, to measure the electrophysiological changes occurring in the smooth muscle cells of the submaxillary gland blood vessels (arterioles) in the cat.

The second objective of this work was to measure the blood flow changes occurring in the submaxillary gland of the cat as a result of parasympathetic nerve stimulation. The measurements of the blood flow changes were to be done utilizing the flow meter described in the first part of this thesis. In the measurement of blood flow particular emphasis was placed on the time course of blood flow changes.

5.3 Methods

5.3A Animals and Anaesthesia

Cats weighing 2 to 4 kg. were used. Anaesthesia was induced by chloroform, aerated with 100% oxygen in a closed box. Ether on a face mask was used for temporary maintenance of anaesthesia until a venous cannula was inserted. Anaesthesia was maintained throughout the experiment by chloralose (80 mg/kg. I.V.).

5.3B Nerve Stimulation

(a) Parasympathetic

The parasympathetic nerve supply to the submaxillary gland runs in the chorda tympani nerve which is a branch of the chorda lingual nerve. The chorda lingual nerve was exposed in the region where it crosses the submaxillary and sublingual ducts, and was cut as near as possible to its point of exit from the skull.

(b) Sympathetic

The cervical sympathetic nerve could readily be exposed and cut in the neck where it runs alongside the vagus nerve.

5.3C Salivary Flow

The submaxillary duct was exposed in the floor of the mouth through the neck, lying medially to the sublingual duct. The submaxillary duct was cannulated with a fine glass cannula, about 5 - 10 mm. rostral to the point

at which the duct was crossed by the chorda lingual nerve.
Flow of saliva in the cannula, upon sympathetic or para-
sympathetic nerve stimulation, was used as an indication
of undamaged operation of the nerve supply in both flow
and electrophysiological experiments.

5.3D Blood Flow

The blood flow (venous outflow) through the submax-
illary gland was measured by putting the flow meter (forced
convection) in the external jugular vein. The probe of
the flow meter was inserted into the external jugular by a
double cannulation. All veins draining into the external
jugular vein were tied except that from the submaxillary
gland. The cats were heparinized with sodium heparin
(10 mg/kg. I.V.) and the inside of the probe was siliconiz-
ed with Siliclad (Clay-Adams), (1 part Siliclad to 20 parts
of water) by soaking the inside for 10 minutes. The probe
was then forced-air dried with a heat gun. Figure 17
shows a schematic diagram of the experimental set-up
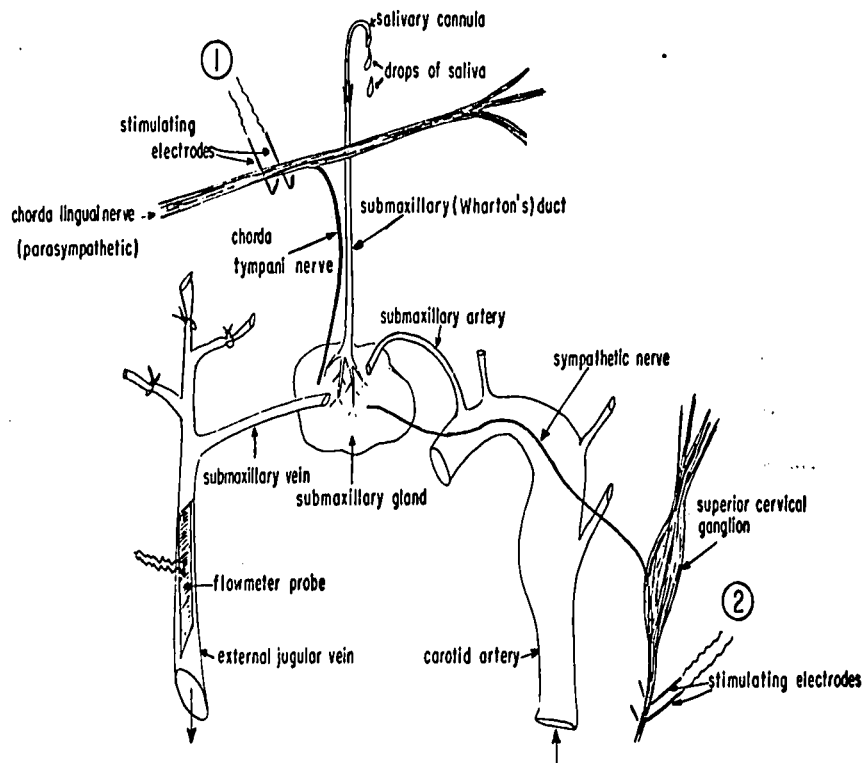used in the blood flow experiments.

Figure 17. Schematic diagram of the experimental set-up
used in the blood flow experiments.

5.3E Electrophysiological Experiments

Cats were anaesthetized using chloroform and maintained on chloralose as for blood flow experiments. The sympathetic and parasympathetic nerve supply and the submaxillary duct were prepared as in the blood flow experiments. The submaxillary gland was dissected out carefully to cause little or no damage to the nerve supply. It was taken out of its capsule and the lobes were separated to expose the blood vessels. This exposed portion of the gland was the part which was posterior to the hilus.

The cat was placed in a Faraday cage. Recordings were made with glass micro-electrodes filled with 3 M potassium chloride and were either fixed, or mounted flexibly on fine platinum wire, and connected to a "Zeiss" micromanipulator. When the electrode was fixed, contact was made with chlorided silver wire. The indifferent electrode was a medicine dropper filled with 0.16 M saline and contact was made using chlorided silver wire. Its tip was placed next to the gland. The resistance of microelectrodes used for the intracellular recording varied from 30 to 55 megohms. The electrodes were connected to a Medistor microelectrode amplifier which had an input impedance of 5×10^4 megohms, an input current of less than 10^{-13} amps, and a band width of 10 to 15 KHz with proper neutralization. The output was fed into a Tektronix 565 storage oscilloscope and results were photographed with a polaroid camera. Stimulation was provided with a Grass

SD5 stimulator or with a Digatimer and, unless otherwise indicated, was set at 20 pulses per second and 7 volts with a pulse width of 0.4 msec. Figure 18 shows a schematic diagram of the experimental set-up used for the electro-physiological experiments.
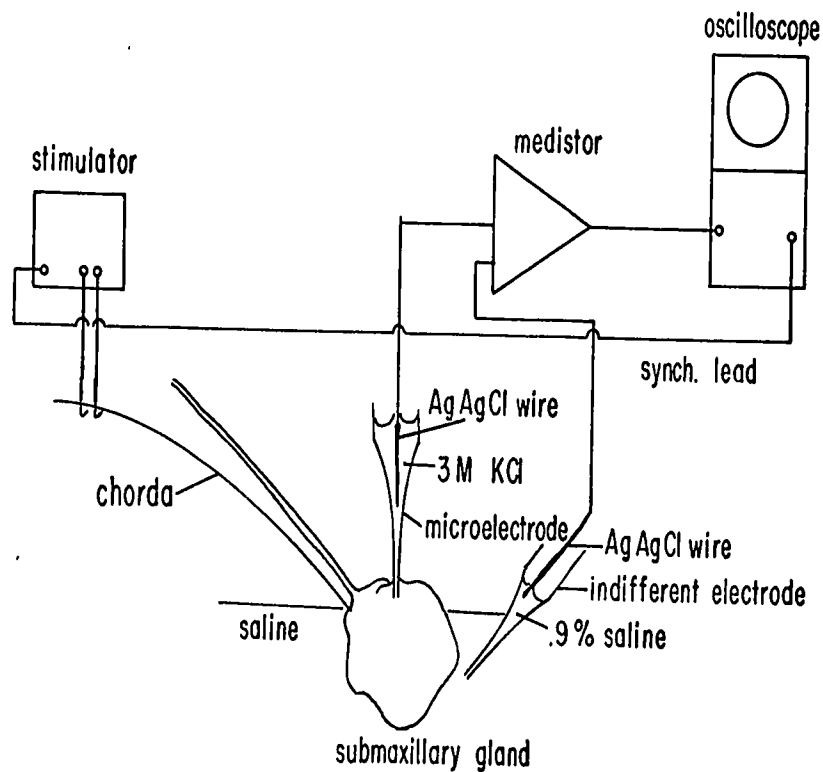

Figure 18. Schematic diagram of experimental set-up used in the electrophysiological experiments.

5.4 Results

5.4A Electrophysiology

Electrophysiological results obtained from secretory cells in the submaxillary gland agree with the results reported by Creed and Wilson (1969). Figure 19 shows a typical response obtained from a secretory cell with a stimulus of 5 pulses to the chorda tympani nerve (parasympathetic). This type of response was the type 1 response described by Lundberg (1955). He showed that it originated from the outer membrane of secretory cells (acinar). The type 1 response as reported by Lundberg, consisted of a resting potential which varied from 15 mV. to 35 mV. and a hyperpolarization response to chorda tympani nerve stimulation of about 20 mV. The latency between chorda stimulation and hyperpolarization was between 200 and 400 msec.

The resting potential of the cell shown in Figure 19 was 40 mV. and the magnitude of the hyperpolarization was 30 mV. The latency was 500 msec. between the beginning of stimulation and the beginning of hyperpolarization.

Secretory cells were also found to respond to a single stimulus of the chorda tympani nerve. A response to a single stimulus of the chorda tympani nerve is shown in Figure 20. The latency was about 350 msec. and the magnitude of the hyperpolarization was about 12 mV. In this cell the resting potential was 40 mV.
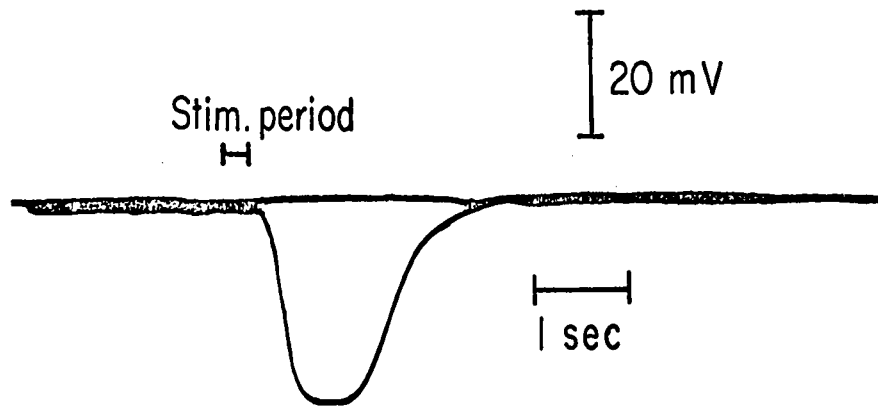
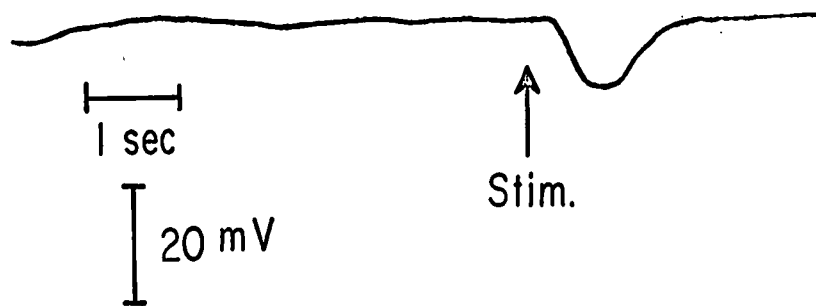Figure 19. Secretory cell response to 5 stimuli of the chorda tympani nerve.

Figure 20. Secretory cell response to a single stimulus of the chorda tympani nerve.

Stimulation of the sympathetic nerve also resulted in a hyperpolarization of secretory cells. This hyperpolarization, as reported by Creed and Wilson (1969), did not occur until the stimulation frequency was nearly 10 stimuli per second and, after an extended period of stimulation, the cells began to depolarize. Lundberg (1955) reported that the sympathetic secretory potential appeared after a longer latency and had a slower rate of hyperpolarization compared to the chorda hyperpolarization. The latency between sympathetic nerve stimulation and hyperpolarization in the submaxillary gland was larger than that observed with chorda tympani nerve stimulation and was nearly a second in some cases. Creed and Wilson reported a mean latency of 662 msec. ± 178 SD at 10 stimuli per second.

A response of a secretory cell to sympathetic nerve stimulation is shown in Figure 21. The latency is approximately 1 second and the magnitude of the hyperpolarization is about 12 mV.

Figure 22 shows the same type of response as shown in Figure 21, but the magnitude of the hyperpolarization response is greater. The latency in this case is about 800 msec. At the end of the trace the microelectrode was taken out of the cell to give an indication of the magnitude of the resting potential and the direction of potential change.
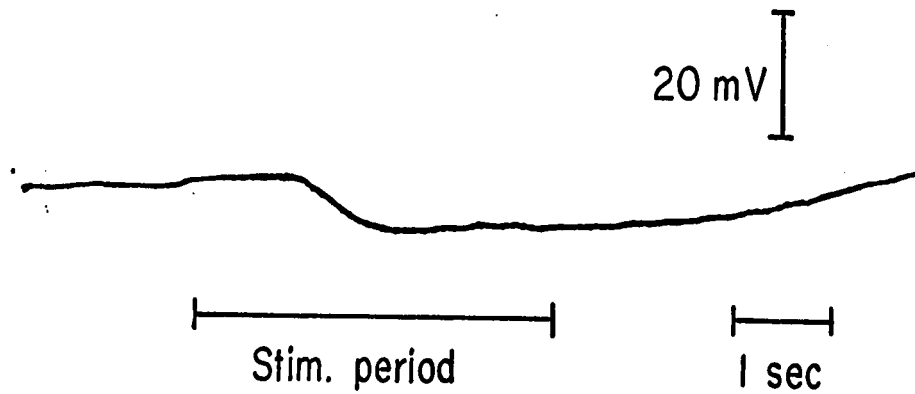
Figure 21. Secretory cell response to sympathetic nerve
stimulation. The sympathetic nerve was stimulated at a
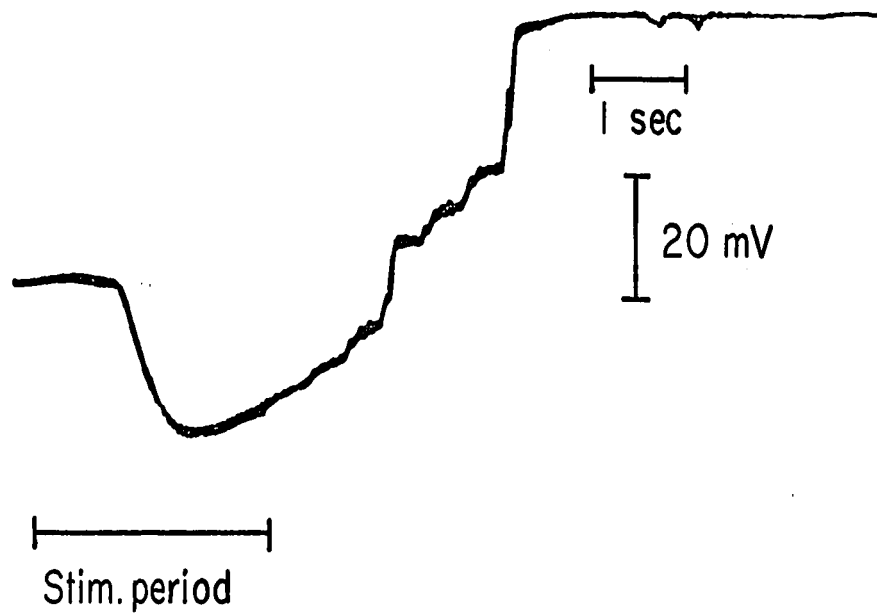frequency of 10 stimuli per second.

Figure 22. Secretory cell response to sympathetic nerve
stimulation. The microelectrode is out of the cell at the
end of the trace.

The electrophysiological results obtained as part of this thesis agree with results obtained by previous workers, Lundberg (1955) and Creed and Wilson (1969). Chorda tympani nerve induced hyperpolarization of secretory cells occurs after a latency of 300 msec., while sympathetic nerve induced hyperpolarization has a longer latency.

The mechanism for the hyperpolarization response has not been established at the present time. An ionic mechanism for the hyperpolarization response has recently been suggested by Petersen and Poulsen (1967, 1968) and Petersen (1970). Petersen (1970) concludes that the hyperpolarization is probably due to an outward potassium current partially short-circuited by an inward sodium current. The potassium equilibrium potential across the basal acinar cell membrane is greater than the maximum hyperpolarization of the cell while the sodium potential is less than the resting membrane potential. Petersen showed that the magnitude of the hyperpolarization increased during perfusion of the gland with potassium-free solution (NaCl) and during perfusion with large non-permeating ions instead of sodium (TEA Cl).

5.4B Blood Flow

Blood flow was measured using the forced convection flow meter. A vasodilatation response of the submaxillary gland to chorda tympani nerve stimulation is shown in

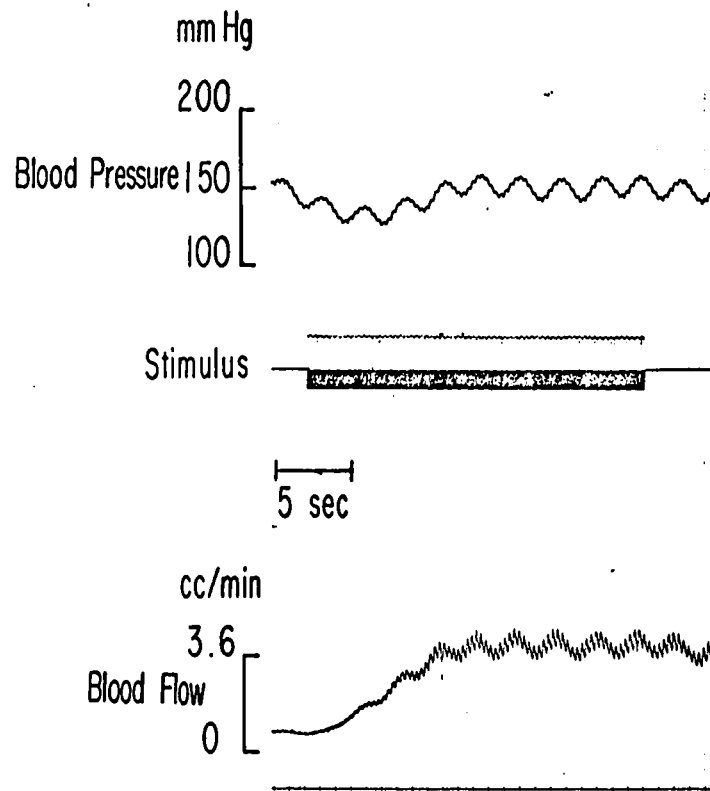Figure 23. The vasodilatation is quick in onset.

Figure 23. Vasodilatation in the cat submaxillary gland as a result of chorda tympani nerve stimulation. Also shown is the stimulus and blood pressure.

Figure 24 shows the response of submaxillary gland blood flow to sympathetic nerve stimulation. The blood flow decreases after a latency of about 1 sec. and after the stimulation has stopped the blood flow increases to a value greater than the basal flow rate. In a few cases, although this is not evident in Figure 24 , this after-

dilatation exceeds the vasodilatation produced by optimal
stimulation of the chorda tympani. This after-dilatation
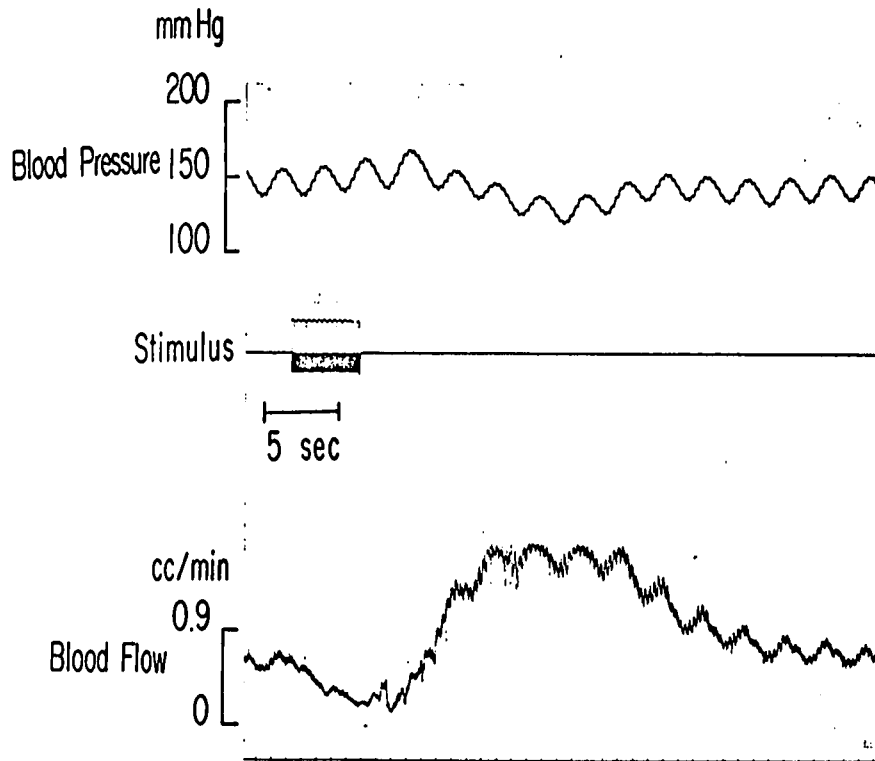was first described by Carlson (1907).

Figure 24. Vasoconstriction in the cat submaxillary
gland as a result of sympathetic nerve stimulation.

In some of the preparations, stimulation of the chorda
tympani nerve with a single stimulus or short pulse trains
elicited vasodilatation. Figure 25 shows the response of
one such gland where volume increase (integral of flow rate)
is plotted versus the number of stimuli. This shows the
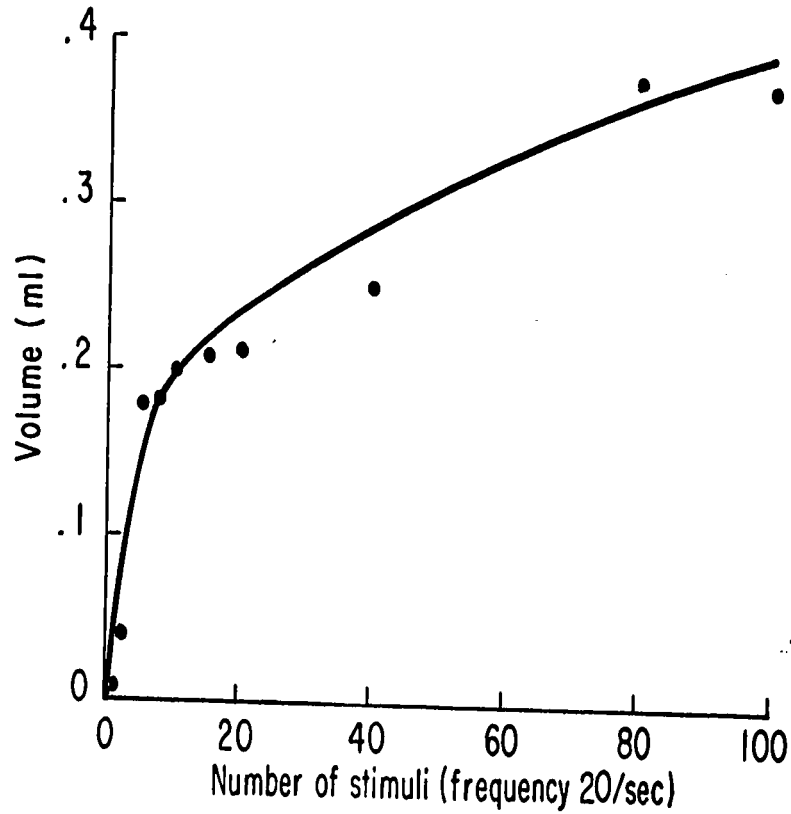
high sensitivity of the measurement system.

Figure 25. Volume increase versus number of stimuli (integral of flow rate). The interval between stimuli was 50 msec. (20/sec.) in cases of more than one pulse.

Latency measurements were made on several different preparations. The latency was taken as the time between the beginning of nerve stimulation and the onset of vasodilatation. One of the shortest latencies is shown in Figure 26. Figure 26A shows the vasodilatation response due to a 3 second period of chorda tympani nerve stimulation. Figure 26B
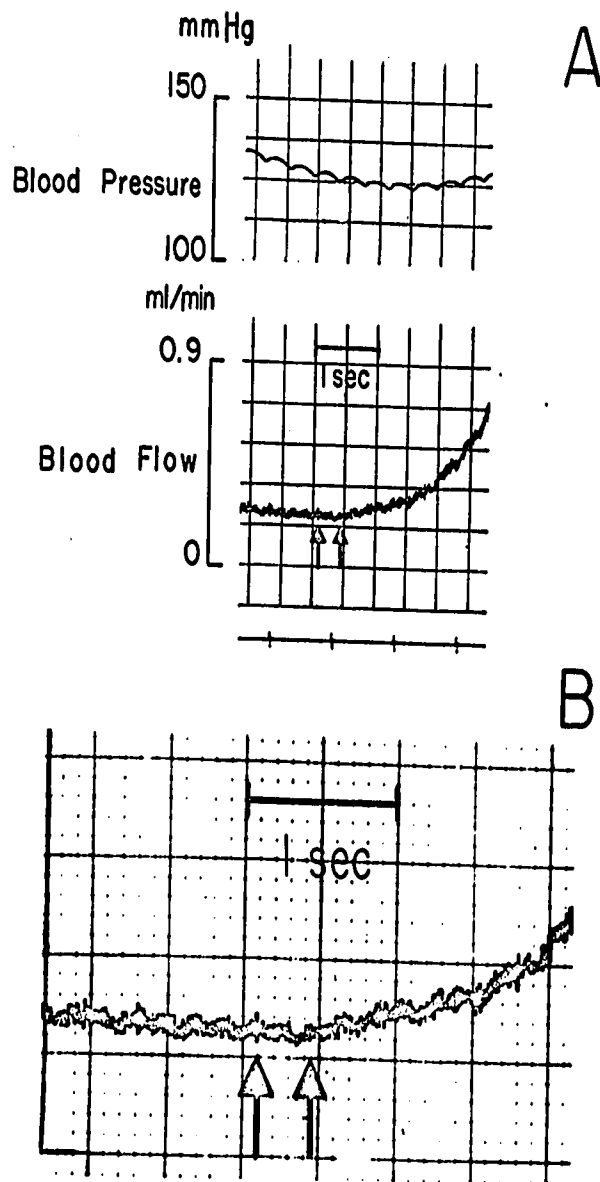
Figure 26. Vasodilatation in the cat submaxillary as a result of a 3 second period of chorda tympani nerve stimulation.

Figure 26A. Blood pressure and blood flow. The first arrow indicates the beginning of stimulation, while the second arrow indicates the onset of vasodilatation.

Figure 26B. Enlarged portion of the vasodilatation response shown in A.

shows an enlarged portion of the vasodilator response.
The latency in this case is 350 msec. or less.

Table 1 gives the shortest latencies measured in five
cats. The means of four measurements in the same animal
are given for experiments 3 and 4. The standard deviations
are also given. In experiments 1, 2 and 5 the values given
are the shortest latencies measured in the experiments. In
these particular experiments only one reasonable measure-
ment of latency was obtained due to experimental difficulties.
Other latencies were usually much longer due to a decrease
in basal flow and general deterioration of the experimental
animal.

Experiment	Shortest Latency (msec.)	Mean Latency (msec.) ± SD
1	800	--
2	900	--
3	550	560 ± 100
4	350	340 ± 55
5	650	--

Table 1. Shortest latencies between chorda tympani nerve
stimulation and onset of vasodilatation.

The onset of vasodilatation was taken as the point at
which a change in slope occured. Straight lines were

fitted to the blood flow record (first order approximation).

The first straight line was fitted to the basal flow portion

of the blood flow record and the second was fitted to the

initial phase of the vasodilatation response. The inter-

section of these straight lines was taken as the onset of

vasodilatation. The latencies obtained in this manner were

compared to those obtained by an unbiased observer from

the same record and were usually larger by 25 msec. or were

of the same magnitude. In experiment 4 latencies were

obtained which were shorter than shown in Figure 26. The

shortest latency obtained in experiment 4 was 250 msec.,

but the vasodilatation was paralleled by an increase in

blood pressure.

The latencies in Table 1 show a wide variation.

However, the most important one is that in experiment 4

since its magnitude is the same as the latency between

chorda tympani nerve stimulation and hyperpolarization of

the secretory cells. This shows that vasodilatation is not

secondary to secretion. Although the latencies in other

experiments exceed the shortest latency, this does not

invalidate the above conclusion.

Some of the variation in latencies shown in Table 1

is probably due to mechanical factors. For example, since

veins are collapsible structures, a change in blood flow at one point does not produce an instantaneous change at a distal point. In the experimental set-up all of the veins, except the submaxillary vein supplying the external jugular are tied off and the vessel is in a partially collapsed state. In vitro measurement on the external jugular vein showed that the time delay between a small pressure change in the submaxillary vein and flow changes at the probe (3 cm. away) was of the order of 50 msec. or more. The basal flow was similar to that shown in Figure 23 and the blood vessel was from the experimental animal listed as cat 3 in Table 1. This time delay measurement is shown in Figure 27.

5.4C Experiments With Bradykinin Potentiating Factor

The synthetic bradykinin potentiating peptide developed by Ferreira, Bartelt and Greene (1970) has the same spectrum of properties as previously reported by Ferreira (1965) for the Bradykinin Potentiating Factor (B.P.F.). The B.P.F. is a peptide fraction from Bothrops jararaca venom which inhibits the enzymes that normally inactivate bradykinin and the enzyme responsible for the conversion of angiotensin I to angiotensin II. The peptide potentiates the depressor effects of bradykinin on blood pressure and also potentiates the effect of bradykinin on capillary permeability.
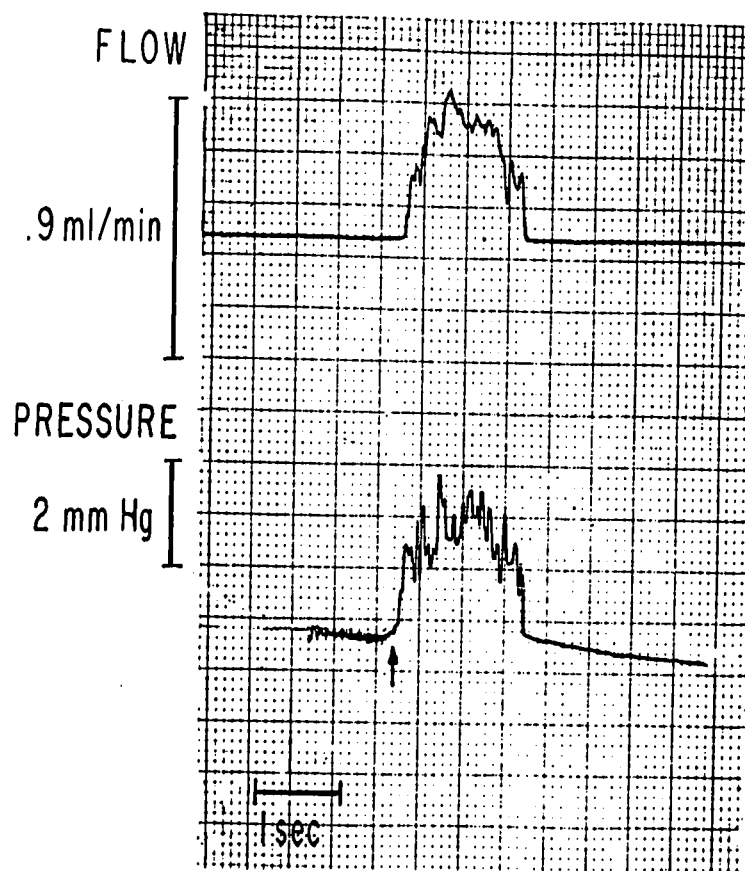
Figure 27. Time delay between pressure change in the submaxillary vein and the resultant flow change in the probe (3 cm. away). The arrow shows the beginning of the pressure pulse.

This experiment is similar to Skinner and Websters' work with carboxypeptidase B. Skinner and Webster (1968) reported that chorda tympani nerve induced vasodilatation was unaffected in cats pretreated with carboxypeptidase B, an inactivator of bradykinin. Skinner and Webster suggested
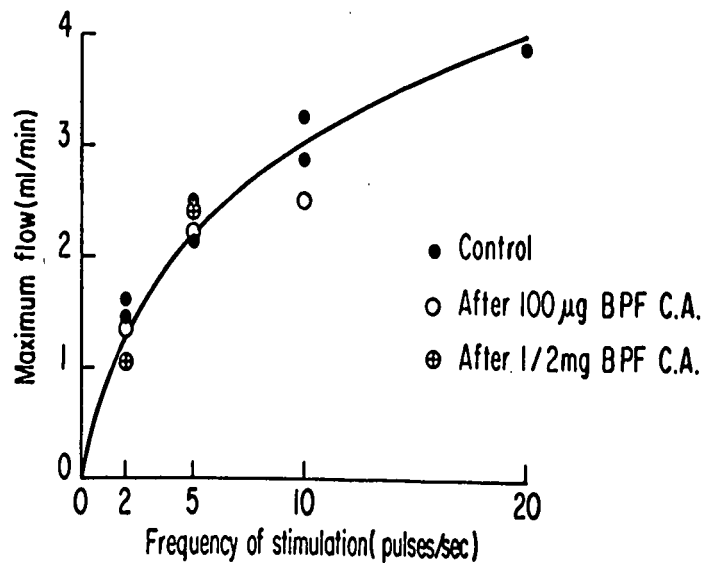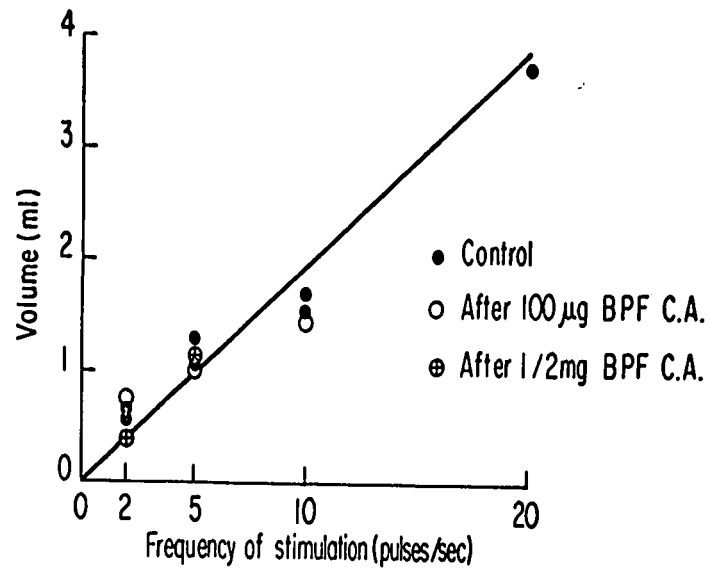
Figure 28. Vasodilatation in the submaxillary gland as a
result of chorda tympani nerve stimulation before and after
B.P.F. B.P.F. was injected close-arterially. The first
curve is a plot of volume increase versus frequency of
stimulation. The second curve is a plot of maximum flow
rate versus frequency of stimulation. The duration of
stimulation was 30 seconds in all cases.

that if chorda tympani nerve induced vasodilatation was
mediated by the kallikrein-kinin system, the response in
animals pretreated with carboxypeptidase B, would be
diminished if not abolished. A similar experiment is one
in which the kallikrein-kinin system is potentiated. A
substance such as B.P.F. which potentiates bradykinin,
should enhance chorda tympani nerve induced vasodilatation
if the kallikrein-kinin system is a mediator. The B.P.F.
was injected close-arterially and no potentiation of
chorda tympani nerve induced vasodilation was observed.
Figure 28 shows a comparison of the two responses before
and after B.P.F. was injected. However, these results are
inconclusive since no vasodilatation could be elicited
with 2 ug of bradykinin injected close-arterially before
the injection of B.P.F. Only one experiment was completed
because of the difficulty in obtaining B.P.F.

The potentiating effect of B.P.F. was easily demon-
strated on the guinea pig ileum. Figure 29 shows the
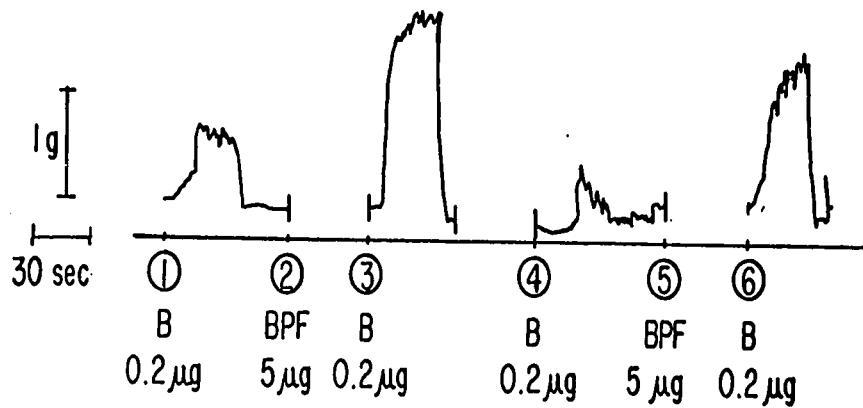response of the guinea pig ileum before and after B.P.F.

Figure 29. Potentiating effect of B.P.F. on the bradykinin response of the guinea pig ileum. At 1, 0.2 ug of brady-kinin was added into the bath. After the response had returned to a control level, 5 ug of B.P.F. was added at 2. Thirty seconds later at 3, 0.2 ug of bradykinin was added. At 4, 5 and 6 the sequence was repeated.

5.5 Discussion

According to Creed and Wilson (1969), the mean
latency between parasympathetic nerve stimulation and
hyperpolarization of the secretory cell, was about 300
msec. at a stimulation frequency of 20 stimuli per second.
Of this, about 60 msec. could be accounted for by nerve
conduction and ganglionic delay, while the greater part
of this latency was attributed to the diffusion of the
transmitter and initiation of hyperpolarization. The
magnitude of the latency between chorda tympani nerve
stimulation and hyperpolarization measured in this work
was the same magnitude as that reported by Creed and
Wilson.

The shortest measured latency between chorda tympani
nerve stimulation and vasodilatation was between 300 and
350 msec. This latency is shorter since a transport
delay exists as was shown in Figure 27. The actual magni-
tude of the transport delay is difficult to estimate.
However, it seems likely that vasodilatation occurs before,
or is simultaneous with, hyperpolarization. In either case,
it seems unlikely that chorda tympani nerve induced
vasodilatation is mediated by the kallikrein-kinin system
or that it is secondary to secretion.

Even in those experiments where the latency is longer
(i.e. 900 msec.), there does not seem to be time for the
kallikrein to act as a mediator of chorda tympani nerve
induced vasodilatation. This mechanism involves the release

of kallikrein from secretory cells, its passage into the interstitial fluid, its action on an α_2-globulin substrate to release kallidin, and the vasodilator action of the kinin on the smooth muscle in the walls of the blood vessels. Although very little is known about the enzyme kinetics involved, in vitro experiments on the guinea pig ileum indicate a slow system.

This view is also held by Gautvik (1970a, b, c). Using a drop counter to measure the venous outflow from the cat submaxillary gland, he estimated the latency between chorda tympani nerve stimulation and onset of vasodilatation to be between 1 and 6 seconds. Gautvik concluded that it seemed unlikely that a mechanism involving release of an enzyme from gland cells, and its successive participation in chemical reaction (s), could be effective within a few seconds. The work in this thesis has shown conclusively that the latency is about 350 msec. or less.

Gautvik suggests that vasodilatation is initiated by nerve fibers, but that the kallikrein-kinin system is also a part of vasodilator response. Thus a nervous mechanism ensures an immediated increase in blood flow, while the kallikrein-kinin system is responsible for the maintenance of blood flow in accordance with metabolic needs. This type of two-phase system was first suggested by Barcroft (1914). His hypothesis was that under normal circumstances dilation may be instituted by dilator fibers and maintained by metabolic products. This was strongly supported by

combined vascular and secretory studies done by Holzlöhner and Hoffman (1931).

A comparison of the latencies which exist when the sympathetic nerve is stimulated, shows that vasoconstriction has a latency of about 1000 msec. and hyperpolarization has a latency of about 650 msec. When the parasympathetic nerve to the gland is stimulated, hyperpolarization of the secretory cells and vasodilatation occur after a latency which is about 300 msec. Since it is generally accepted that vasoconstriction is directly controlled by the sympathetic nerve, the shortness of the latency which precedes parasympathetic vasodilatation, lends support to the theory that parasympathetic vasodilator nerve fibers exist.

Preliminary experiments with B.P.F. showed no potentiation of chorda tympani nerve induced vasodilatation, but since close-arterial injection of bradykinin did not elicit vasodilatation, the results are inconclusive.

The results shown in this work would tend to support the theory that chorda tympani nerve induced vasodilatation is mediated by a direct nervous mechanism. This mechanism would involve the release of a transmitter such as acetylcholine. However, no evidence is available as to the nature of the transmitter or the mechanism involved, nor is it evident at the present time why the vasodilatation is not blocked by moderate doses of atropine if the transmitter is acetylcholine as is suggested by Schachter

and Beilenson (1968).

In order to explain parasympathetic induced vasodilatation after atropine, Gautvik (1970c) has postulated two neuro-effector mechanisms. One mechanism controls the release of kallikrein from secretory cells and the other one acts directly on the resistance vessels. Both postulated mechanisms are atropine resistant.

The results of this thesis quite conclusively rule out the possibility that the kallikrein-kinin system plays a role in the initial phase of chorda tympani nerve induced vasodilatation, but they do not reveal anything about the possibility that maintained vasodilatation is mediated by a metabolic product, as is suggested by Barcroft (1914), Holzlöhner and Hoffman (1931) and Gautvik (1970a, b, c).

The only method which would conclusively show the existence of parasympathetic vasodilator fibers is electrophysiological recording from smooth muscle cells in the walls of blood vessels. If successful, the latency of the electrical response of vascular smooth muscle would give a final answer to the question of whether parasympathetic vasodilator nerve fibers exist or not in the submaxillary gland of the cat.

Some work which applies to this type of problem has been reported. Funaki (1958, 1960, 1961) recorded resting membrane potentials and action potentials in smooth muscle cells in the blood vessels of the tongue and abdominal skin of the frog. Funaki (1961) reported resting membrane

potentials of about 40 mV and spike potentials of 60 mV.

in magnitude and 200 msec. in duration. He also reported

that the resting potential of endothelial cells was about

47 mV with no action potentials present.

Steedman (1966) has also reported recent work in this

area. He used as one of his preparations the smooth muscle

cells in the walls of small arteries in the tongue and skin

of the lateral abdomen in the frog. Another preparation

used by Steedman was the smooth muscle cells in the walls

of small arteries and arterioles of the rat mesenteric

circulation. He reported resting potentials with mean

values of 64.7 mV in the frog tongue and 43.6 mV in the

skin of the lateral abdomen. Action potentials of up to

60 mV in amplitude and 100 - 200 msec. in duration could

be elicited by electrical stimulation of the blood vessel

wall in a position near the recording electrode. This

result was reported in the frog tongue blood vessels.

In the work by Steedman on the rat mesenteric circu-

lation, intracellular potentials varied continually with a

maximum polarization of 39.4 mV. The slow waves had

periods varying from 4.7 - 7.8 seconds. Spike potentials

were recorded with amplitudes of up to 35 mV and durations

varying from 40 - 50 msec. Steedman also reported that

interference with the autonomic nervous system, chemically

or by denervation, affected the amplitude of slow waves

but not the frequency and occurrence of the action poten-

tials. Stimulation of the smooth muscle cells by electri-

cal stimulation of the splanchnic nerves and local application of adrenalin, noradrenalin and vasopressin increased the frequency of action potentials and the amplitude of the slow waves, while acetylcholine and removal of the nerve supply depressed the electrical activity.

The work of Funaki and Steedman indicates that if nerve activity could be related to smooth muscle activity (blood vessels) in the salivary gland, the question of whether parasympathetic vasodilator nerves exist would be answered.

This work is in progress at the present time with very little success. Due to the small size of the muscle cells and difficulties with the connective tissue the measurements are proving difficult.

5.6 Conclusions

(1) Chorda tympani nerve induced vasodilatation occurs before, or at the same time as, hyperpolarization of secretory cells.

(2) The initial phase of chorda tympani nerve induced vasodilatation is not mediated by the kallikrein-kinin system.

Bibliography

Barcroft, J. (1914). "The respiratory function of the blood". Cambridge University Press. London.

Barcroft, J. and Müller, F. (1912). The relation of blood flow to metabolism in the submaxillary gland. *J. Physiol*. 44, 259.

Barcroft, J. and Piper, H. (1912). The gaseous metabolism of the submaxillary gland with reference especially to the effect of adrenalin and the time relation of the stimulus to the oxidation process. *J. Physiol*. 44, 359.

Bayliss, W.M. (1923). "The Vasomotor System". Longmans, Green and Co., New York.

Bayliss, W.M. and Bradford, J.R. (1886). The electrical phenomena accompanying the process of secretion in the salivary glands of the dog and cat. *Proc. Roy. Soc*. 40, 203.

Beilenson, S., Schachter, M. and Smaje, L.H. (1965). Kallikrein in the submaxillary gland of the cat. *J. Physiol*. 177, 61P.

Beilenson, S., Schachter, M. and Smaje, L.H. (1968). Secretion of kallikrein and its role in vasodilatation in the submaxillary gland. *J. Physiol*. 199, 303.

Bernard, C. (1858). De l'influence de deux ordres de nerfs qui determinent les variations de couleur du sang veineux dans les organes glandulaires. *C.R. Acad. Sci.* 47, 245.

Bhoola, K.D., Morley, J., Schachter, M. and Smaje, L.H. (1965). Vasodilatation in the submaxillary gland of the cat. *J. Physiol.* 179, 172.

Boussinesq, M.J. (1905). Calcul du pouvoir refroidissant des courants fluides. *J. de Math.* 1, 285.

Bradford, J.R. (1887). The electrical phenomena accompanying the excitation of so called secretory and trophic nerve fibres in the salivary glands of the dog and cat. *J. Physiol.* 8, 86.

Carlson, A.J. (1907). Vasodilator fibres to the submaxillary gland in the cervical sympathetic of the cat. *Amer. J. Physiol.* 19, 408.

Corrsin, S. (1963). Turbulence: Experimental methods. In *Encyclopedia of Physics* , ed. Flügge, S., p. 524. Springa-Verlag, Berlin VIII/2.

Creed, K.E. and Wilson, J.A.F. (1969). The latency of response of secretory acinar cells to nerve stimulation in the submandibular gland of the cat. *Aust. J. Exp. Biol. Med. Sci.* 47, 135.

Davey, M.J., Davies, R.F., Reinert, H. and Scholfield, P. (1965). Effects of adrenergic-neurone blocking agents on the submaxillary gland of the cat. *Nature.* 205, 673.

Ferreira, S.H. (1965). A bradykinin-potentiating factor (BPF) present in the venom of Bothrops jararaca. *Brit. J. Pharmacol. Chemother.* 24, 163.

Ferreira, S.H., Bartelt, D.C. and Greene, L.J. (1970). Isolation of bradykinin potentiating peptides from Bothrops jararaca. *Biochem.* In Press.

Funaki, S. (1958). Studies on membrane potentials of vascular smooth muscle with intracellular micro-electrodes. *Proc. Japan Acad.* 34, 534.

Funaki, S. (1960). Electrical activity of single vascular smooth muscle fibres. In *Electrical Activity of Single Cells*. Tokyo: Igakushoin; Hongo.

Funaki, S. (1961). Spontaneous spike-discharge of vascular smooth muscle. *Nature, Lond.* 191, 1102.

Garrett, J.R. (1966c). The innervation of salivary glands. III. The effect of certain experimental procedures on the cholinesterase-positive nerves in glands of the cat. *J. roy. micr. Soc.* 86, 1.

Garrett, J.R. (1966d). The innervation of salivary glands. IV. The effects of certain experimental procedures on the ultrastructure of nerves in glands of the cat. *J. roy. micr. Soc.* 86, 15.

Gautvik, K. (1970a). Studies on kinin formation in functional vasodilatation of the submandibular salivary gland in cats. *Acta physiol. scand.* 79, 174.

Gautvik, K. (1970b). The interaction of two different vasodilator mechanisms in the chorda-tympani activated submandibular salivary gland. *Acta physiol. scand.* 79, 188.

Gautvik, K. (1970c). Parasympathetic neuro-effector transmission and functional vasodilatation in the sub-mandibular salivary gland of cats. *Acta physiol. scand.* 79, 204.

Grahn, A.R., Paul, M.H. and Wessel, H.U. (1968). Design and evaluation of a new linear thermistor velocity probe. *J. Appl. Physiol.* 24, 236.

Grahn, A.r., Paul, M.H. and Wessel, H.U. (1969). A new direction sensitive probe for catheter-tip thermal velocity measurements. *J. Appl. Physiol.* 27, 407.

Heidenhain, R. (1872). Ueber die Wirkung einiger Gifte auf die Nerven der glandula submaxillaris. *Arch. ges. Physiol.* 5, 309.

Hilton, S.M. (1960). Plasma kinin and blood flow. In *Polypeptides which affect smooth muscles and blood vessels*, ed. Schachter, M., p 326. Pergamon Press, London.

Hilton, S.M. (1962). Local mechanisms regulating peripheral blood flow. *Physiol. Rev. Supp.* 5, 265.

Hilton, S.M. (1963). A discussion of the evidence for kinins as the agents of vasodilator reactions. *Anns. N.Y. Acad.* 104, 275.

Hilton, S.M. (1970). The physiological role of glandular kallikreins. In *Handbook exp Pharmacol.* p 389.

Hilton, S.M. and Lewis, G.P. (1955a). The cause of the vasodilatation accompanying activity in the submandibular gland. *J. Physiol.* 128, 235.

Hilton, S.M. and Lewis, G.P. (1955b). The mechanism of the functional hyperaemia in the submandibular salivary gland. *J. Physiol.* 129, 253.

Hilton, S.M. and Lewis, G. P. (1956). The relationship between glandular activity, bradykinin formation and functional vasodilatation in the submandibular salivary gland. *J. Physiol.* 134, 471.

Hilton, S.M. and Lewis, G.P. (1957). Functional vasodilatation in the submandibular salivary gland. *Brit. Med. Bull.* 13, 189.

Hilton, S.M. and Lewis, G.P. (1958). Vasodilatation in the tongue and its relationship to plasma kinin formation. *J. Physiol.* 144, 532.

Hilton, S.M. and Torres, S. H. (1967). Bradykinin and functional vasodilatation in the submandibular salivary gland in the cat. *J. Physiol.* 189, 69P.

Hinze, J.O. (1959). "Turbulence". Mc Graw-Hill., New York-Toronto-London.

Holzlöhner, E. and Hoffman, F. (1931). Die Drüsentätigkeit bei Nervenreizung. II. Die Beziehungen zwischen Blutstrom und Sekretstrom der Glandula submaxillaris bei Chordareizung. *Z. Biol.* 91, 552.

James, G.W., Paul, M.H. and Wessel, H.U. (1966). Thermal dilution: instrumentation with thermistors. *J. Appl. Physiol.* 21, 1131.

Janssen, J.M.L., Ensing, L. and Van Erp, J.B. (1959). A constant-temperature operated hot wire anemometer. *Proc. I.R.E.* 47, 555.

Katsura, S., Weiss, R., Baker, D. and Rushmer, R.F. (1959). Isothermal blood flow velocity probe. *I.R.E. Trans. Med. Elec.* 6, 283.

King, L.V. (1914). On the convection of heat from small cylinders in a stream of fluid: determination of the convection constants of small platinum wires with application to hot wire anemometry. *Phil. Trans. Roy. Soc. Lond.* A214, 373.

Kudryashev, L.I. and Smirnov, A.A. (1965). Estimation of influence of thermal unsteady state on connective heat transfer coefficient for spherical bodies in flow at small Reynold's numbers. *Proc. of the Second All-Soviet Union Conference of Heat and Mass Transfer.* 1, 343.

Kuntz, A. and Richins, C.A. (1946). Components and distribution of the nerves of the parotid and submandibular glands. *J. comp. neurol.* 85, 21.

Landau, L.D. and Lefshitz, E.M. (1959). "Fluid Mechanics". Pergamon Press, London.

Lewis, G.P. (1960). Active polypeptides derived from plasma proteins. *Physiol. Rev.* 40, 647.

Lewis, G.P. (1962). Pharmacological actions and function of bradykinin. *Biochem. Pharmacol.* 10, 29.

Lewis, G.P. (1963). Pharmacological actions of bradykinin and its role in physiological and pathological reactions. *Ann. N.Y. Acad. Sci.* 104, 236.

Lundberg, A. (1955). The electrophysiology of the submaxillary gland of the cat. *Acta physiol. scand.* 35, 1.

Lundberg, A. (1957a). Secretory potentials in the sublingual gland of the cat. *Acta physiol. scand.* 40, 21.

Lundberg, A. (1957b). The mechanism of establishment of secretory potentials in sublingual gland cells. *Acta physiol. scand.* 40, 35.

Lundberg, A. (1957c). Anionic dependence of secretion and secretory potentials in the perfused sublingual gland. *Acta physiol. scand.* 40, 101.

Lundberg, A. (1958). Electrophysiology of salivary glands. *Physiol. Rev.* 38, 21.

Ludwig, C. (1851). Neue Versuche über die Beihilfe der der Nerven zur Speichelabsonderung. *Z. rat. Med. N.F.* 1, 255.

Morley, J., Schachter, M. and Smaje, L.H. (1966). Vasodilatation in the submaxillary gland of the rabbit. *J. Physiol.* 187, 595.

Petersen, O.H. (1970). Transmembrane secretory potentials in the cat submandibular gland during perfusion with potassium-free and low sodium Locke solutions. *Experientia.* 26, 612.

Petersen, O.H. and Poulsen, J.H. (1967). The effects of varying the extracellular potassium concentrations on the secretory rate and on resting and secretory potentials in the perfused cat submandibular gland. *Acta physiol. scand.* 70, 243.

Petersen, O.H. and Poulsen, J.H. (1968). Secretory potentials, potassium transport and secretion in the cat submandibular gland during perfusion with sulfate Locke's solution. *Experientia.* 24, 919.

Prasad, K. and Mac Leod, D.P. (1966). Effect of hemi-cholinium no. 3 on the response of frog rectus abdominus muscle to acetylcholine. *Can. J. Physiol. Pharmacol.* 44, 179.

Rasmussen, R.A. (1962). Application of thermistors to measurements in moving fluids. *Rev. Sci. Instr.* 33, 38.

Richardson, K.C. (1964). The fine structure of the albino rabbit iris with special reference to the identification of adrenergic and cholinergic nerves and nerve endings in its intrinsic muscle. *Am. J. Anat.* 114, 173.

Schachter, M. and Beilenson, S. (1967). Kallikrein and vasodilatation in the submaxillary gland. *Gastro-enterology.* 52, 401.

Schachter, M. and Beilenson, S. (1968). Mediator of vasodilatation in the submaxillary gland. *Federation Proc.* 27, 73.

Skinner, N.S. and Webster, M.E. (1968). Submaxillary gland blood flow: the role of kinins and beta-adrenergic receptors. *Federation Proc.* 27, 76.

Snell, R.S. and Garrett, J.R. (1958). The effect of postganglionic sympathectomy on the histochemical appearances of cholinesterase in the nerves supplying the submandibular and sublingual salivary glands of the rat. *Zeitschrift für Zellforschung.* 48, 201.

Steedman, W.M. (1966). Micro-electrode studies on mammalian vascular muscle. *J. Physiol.* 186, 382.

Strömblad, B.C.R. and Dresel, P.E. (1963). Experiments on atropine-resistant vasodilatation in salivary glands. *Can. J. Biochem. Physiol.* 41, 519.

Terroux, K.G., Sekelj, P. and Burgen, A.S.V. (1959). Oxygen consumption and blood flow in the submaxillary gland of the dog. *Can. J. Biochem. Physiol.* 37, 5.

Ungar, G. and Parrot, J.L. (1936). Sur la présence de la callicréine dans la salive, it la possibilité de son intervention dans la transmission chiminque de l'influx nerveux. *C. R. Soc. Biol. Paris.* 122, 1052.

Werle, E. and Von Roden, P. (1936). Uber das Vorkommen von Kallikrein in den Speicheldrüsen und im Mund-speichel. *Biochem. Z.* 286, 213.

Ziegler, M. (1934). "The Construction of a Hot-Wire Anemometer with Linear Scale and Negligible Lag". Laboratorium voor Aerodynamica et Hydrodynamica der Technische Hogeschool te Delft, in Verhandelingen der Kon. Ned. Akadamie van Wetenschappen te Amsterdam, Afdeling Natuurkunde, Mededeling 29.

Appendix 1   ACHIEVED SPECIFICATIONS

The flow meter, as described in Chapters 2, 3 and 4, was more than adequate for use in measuring the venous outflow from the submaxillary gland.

(1) Flow sensitivity--measures less than 0.05 ml./min. (0.08 cm./sec. in 1.6 mm. probe).

(2) Bandwidth at zero velocity estimated 125 Hz to increasing and decreasing velocity (increases with increasing velocity).

(3) Noise--less than 0.5 mV r.m.s. referred to the input of the squaring circuit (zero velocity).

--0.6 mV r.m.s. referred to the input of the squaring circuit (velocity 0.4 cm./sec.).

Sensitivity is a factor of 100 times greater than that achieved by electromagnetic or ultrasonic techniques. The bandwidth is much higher than that achieved with the drop counter or thermistors and thermocouples operated in the constant current mode.

Appendix 2   CIRCUITS

A2.1 General Scheme

    A block diagram showing the arrangement of the forced

convection flow meter is shown in Figure A-1. This is the

same as is shown in Figure 7.
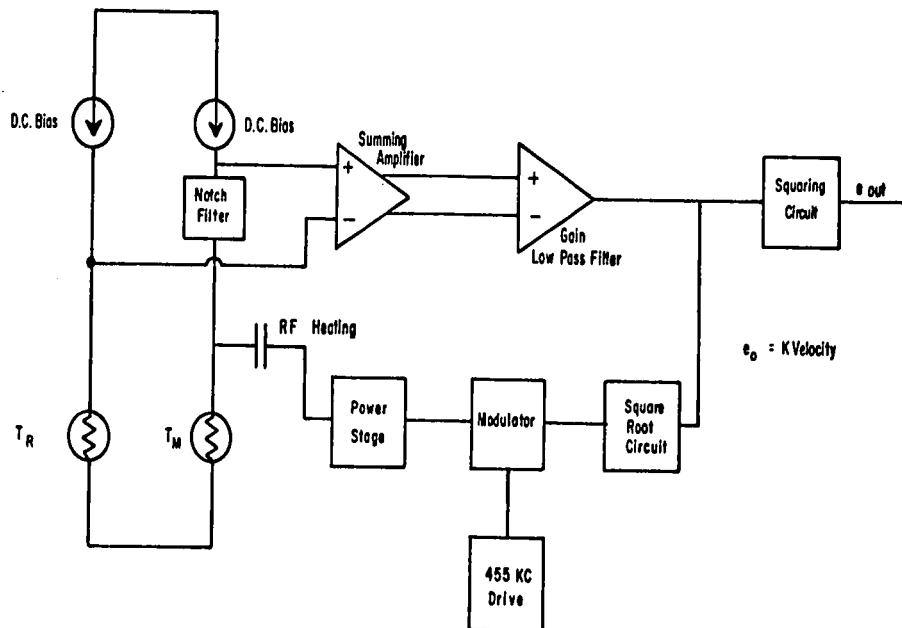
Figure A-1. Block diagram of flow meter.

A2.2 Heating Circuit

    The heating circuit which is the 455 KHz drive, the

modulator and the power stage shown in Figure A-1 is shown

in block diagram form in Figure A-2. The heating circuit

starts with a 910 KHz sine wave drive and the resulting RF

power is a 455 KHz sine wave.
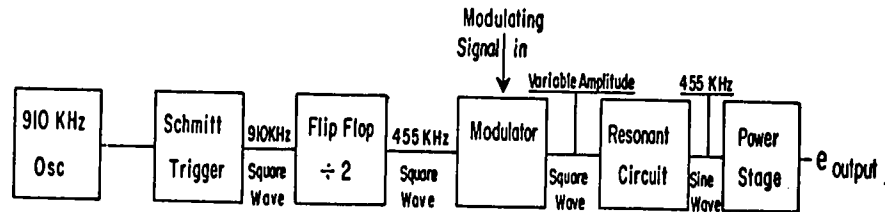
Figure A-2. Block diagram of heating circuit.

A2.2a Oscillator

The oscillator provides the basic 910 KHz drive for

the heating circuit. A slug tuner allows the frequency to

be set. The frequency stability of the oscillator is

quite good. The circuit diagram is shown in Figure A-3.

A2.2b Schmitt Trigger and Flip Flop

The output from the oscillator drives a Fairchild 914

integrated circuit connected as a Schmitt trigger. This

results in a 910 KHz square wave which varies from 0 to

+3.6 volts. The output from the Schmitt drives a binary

scaler. This binary scaler is a Fairchild 923 integrated

circuit used as a counting flip flop. The output is a 1.5 v

455 KHz square wave.
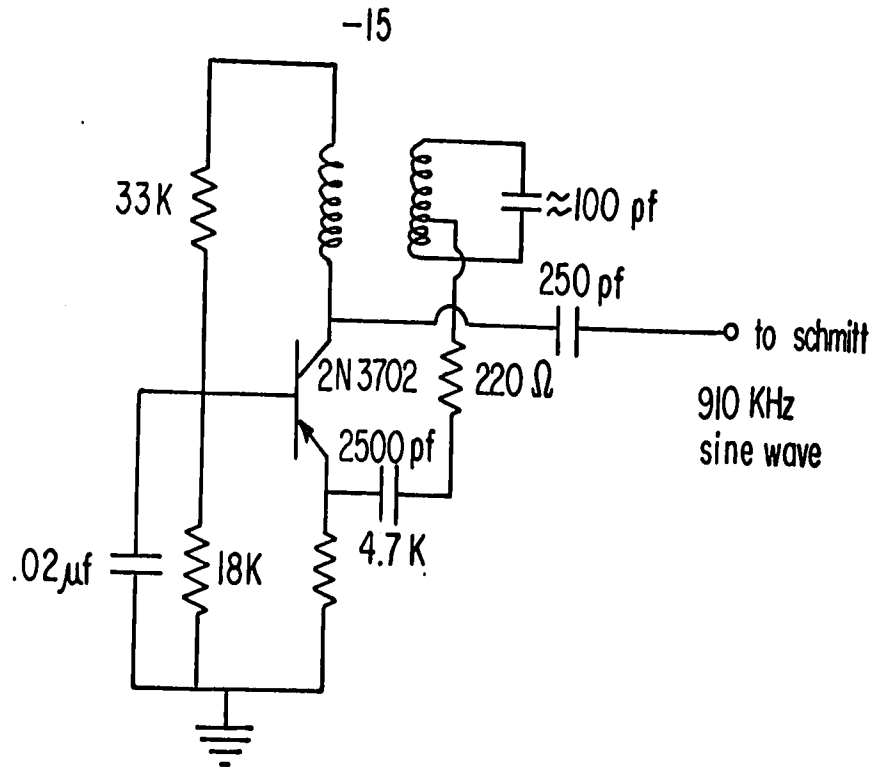
Figure A-3. Oscillator.

A2.2c Modulator

The output from the flip flop drives a switching
transistor in and out of saturation. The square wave
amplitude of the collector output is controlled by the
variation of the supply voltage to the switching transistor.
This is done by the modulating signal via the two emitter
followers. This technique gives very linear amplitude
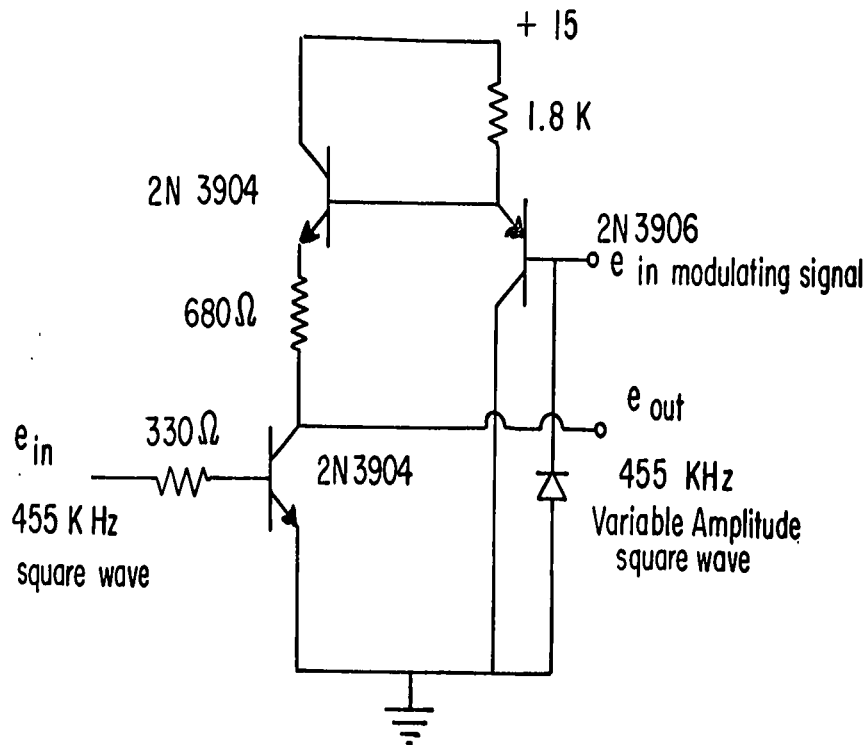modulation. The circuit diagram of the modulator is shown
in Figure A-4.

Figure A-4. Modulator.

A2.2d Resonant Amplifier

This amplifier converts the 455 KHz amplitude modulated
square wave into a 455 KHz amplitude modulated sine wave.
This is done by filtering out the harmonics so as to
simplify the filtering procedure in the detecting system.
This filtering can be done by using another resonant filter.
The resistor across the coil is adjusted to load it in
order to prevent it from over-driving the power stage. The
circuit diagram of the resonant amplifier is shown in
Figure A-5.
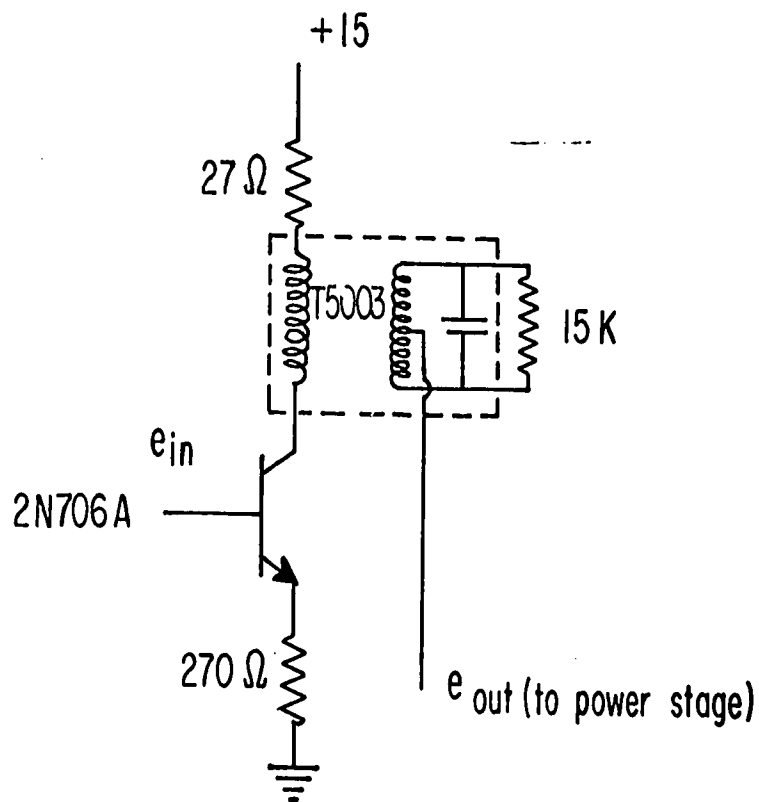
Figure A-5. Resonant amplifier.

A2.2e Power Stage

This stage provides the power to heat the measuring
thermistor. It has the capability to provide almost ½ watt
at 455 KHz. At zero flow it provides about 8 mw. to heat
the thermistor above the ambient temperature of the blood.
The RF power is coupled to the thermistor through a
capacitor. The diodes bias the transistors so that they are
turned on when the input is zero. This prevents cross-over
distortion. The small resistors in series with the col-
lectors and bases of the power transistors protect the

transistors against overload. The circuit diagram is shown
in Figure A-6.
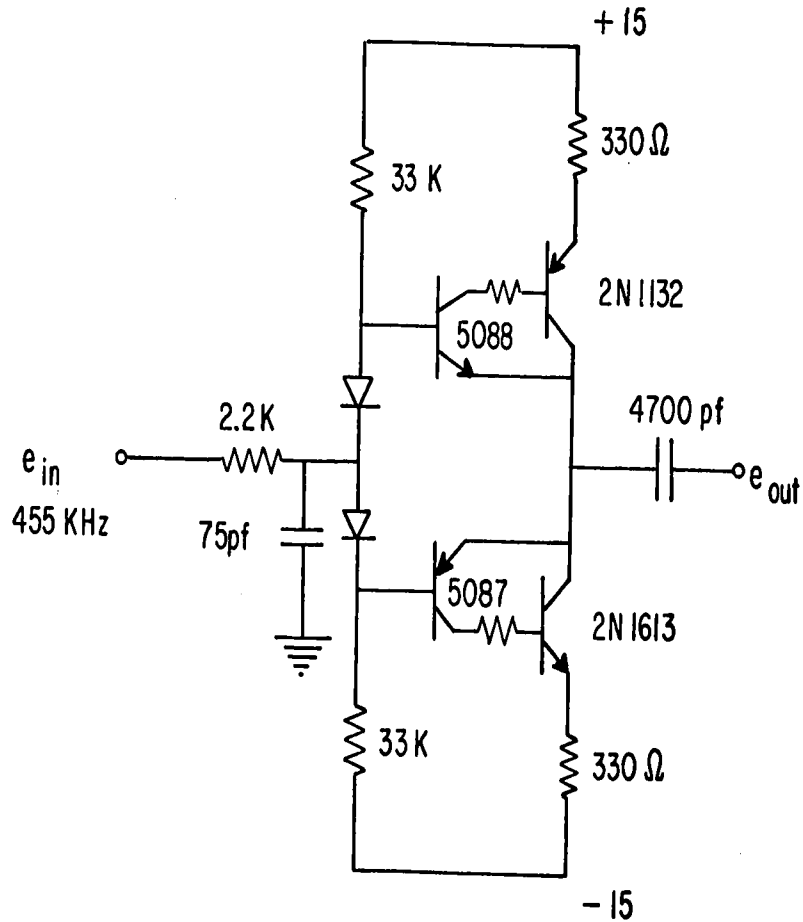
Figure A-6. Power stage.

A2.3 Measuring Thermistor and Filter

The measuring thermistor was biased with a D.C.
current of about 100 ua. This current through the thermistor
resulted in a small voltage across the thermistor and hence
changes in the resistance of the thermistor due to cooling
were converted to voltage changes. The heating power was

filtered by the LC filter at the input of the amplifier.
Additional filtering was provided by the 0.02 uf capacitor.
The circuit diagram of the scheme is shown in Figure A-7.
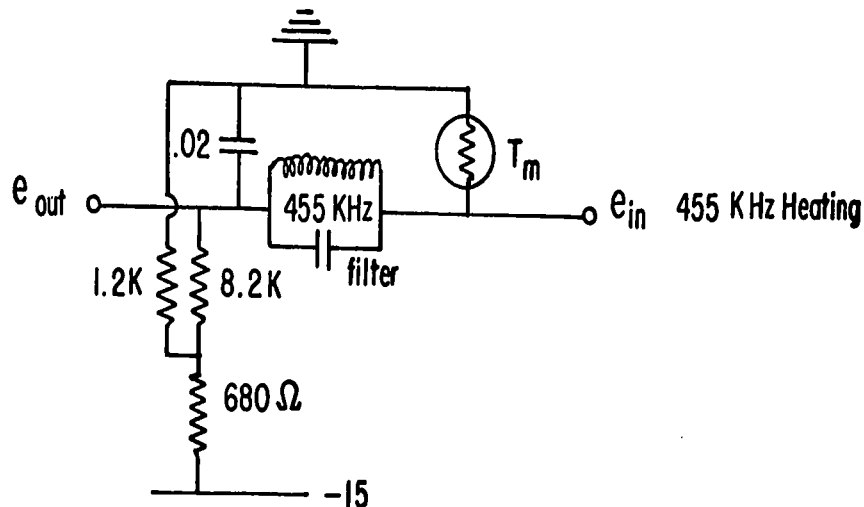
Figure A-7. Measuring thermistor and filter.

A2.4 Compensating Thermistor

This thermistor provides the zero flow balance for
the system and also the compensation for temperature changes
of the blood. The D.C. bias is about 30 - 50 uamps so that
the voltage drop across the heated and reference thermistor
is the same at zero flow. When the flow is not zero, the
voltage across the reference thermistor does not change
since it is insensitive to flow. A resistor (in the probe)
balances the two temperature coefficients of resistance.
The capacitor filters any heating power that may be present

in the thermistor due to coupling through the fluid. A circuit diagram is shown in Figure A-8.
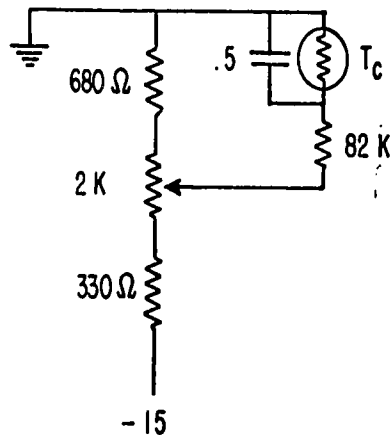

Figure A-8. Compensating thermistor.

A2.5 Amplifier

Since 455 KHz loads integrated circuit operational amplifiers, a discrete component amplifier was used as the input stage. The output amplifier was an integrated circuit operational amplifier. The voltage gain of this combination was 10^4. The input stage was a temperature controlled differential pair of closely matched transistors. The drift of this combination was about 1 uV/degree C. The input stage was operated at a reduced supply voltage to improve noise performance. The operating current set

by the temperature compensated current source was set at
90 uamps for optimal noise performance and current gain.
Protection diodes were also included in the input stage.

The input resistances of the second stage were
adjusted so that the loading on the first stage was bal-
anced. The feedback resistor of the second stage was
split to give a gain of 100. This splitting was necessary
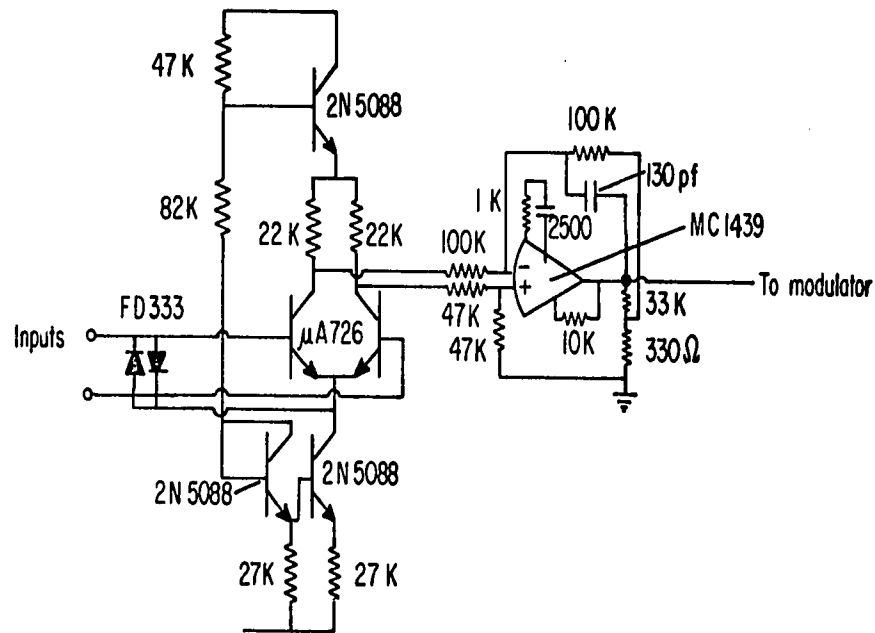so that a smaller feedback resistor could be used. Figure
A-9 shows a circuit diagram of the amplifier circuit.

Figure A-9. Amplifier.

A2.6 Linearizing Circuits

A2.6a Square Root Circuit

This circuit was placed in the feedback path to compensate for the non-linearity due to the second power of current in Joule's Law. This circuit consists of two operational amplifiers; the first generating the non-linearity while the second provides the bias which heats the measuring thermistor above the ambient temperature of the blood. The second amplifier gain is less than one so that the non-linear amplifier can operate over a 10 volt range. It incorporates a compensator. The non-linearity is generated by turning the diodes on and decreasing the feedback resistance. The first diode turns on at about 0.5 volts and the second turns on at about 1 volt. All the other diodes turn on at 1 volt intervals set by the 33 ohm resistors. The non-linearity is generated so that 10 volts at the input results in 10 volts at the output. The 240 K and 360 K resistors were adjusted to give the correct value of gain and power bias. A schematic diagram of the square root circuit is shown in Figure A-10 and of the diode network in Figure A-11.

A2.6b Squaring Circuit

This circuit provides compensation for the non-linearity due to the heat transfer from the thermistor. The first amplifier provides a variable gain through a range switch to provide variable sensitivities and allow

the output to operate over the major portion of the
generated non-linearity. The range switch varies the flow
sensitivities from 1 to a sensitivity 100 times greater.
The squaring amplifier operates similarly to the square
root circuit except that the diode network is in series
with the input. The first amplifier has a corner frequency
of 160 Hz while the second amplifier has a corner frequency
of 190 Hz. The non-linearity was set so that 10 volts at
the input resulted in a 10 volt output. This was set by
making a fine adjustment in the gain of the first amplifier
(50 ml./min. = 10 V out). Figure A-12 shows a circuit
diagram of the squaring circuit and the range control.
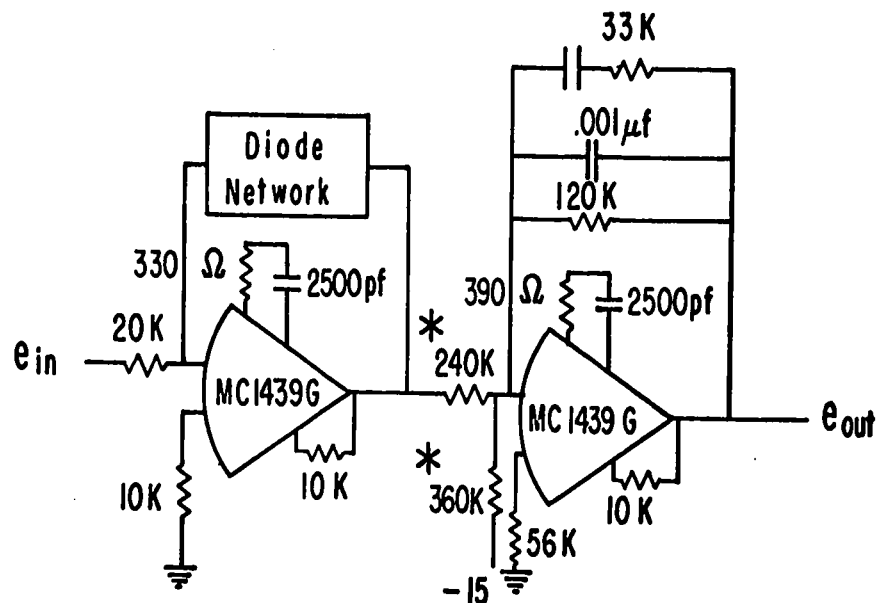Figure A-13 shows a circuit diagram of the diode network.

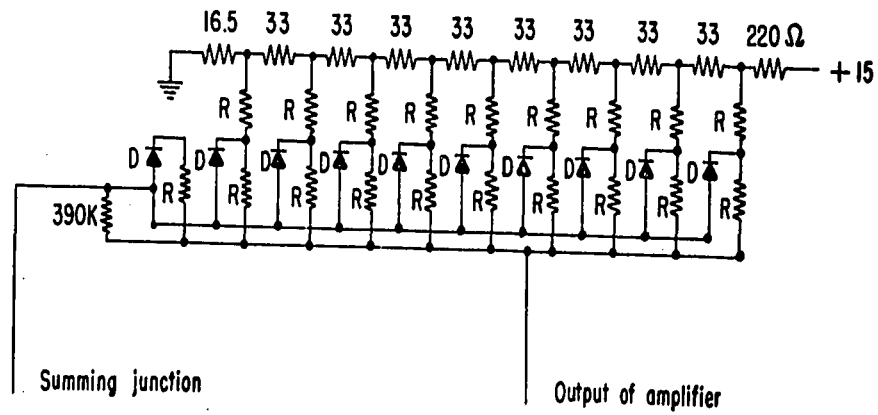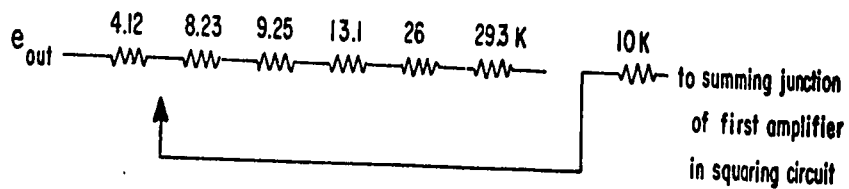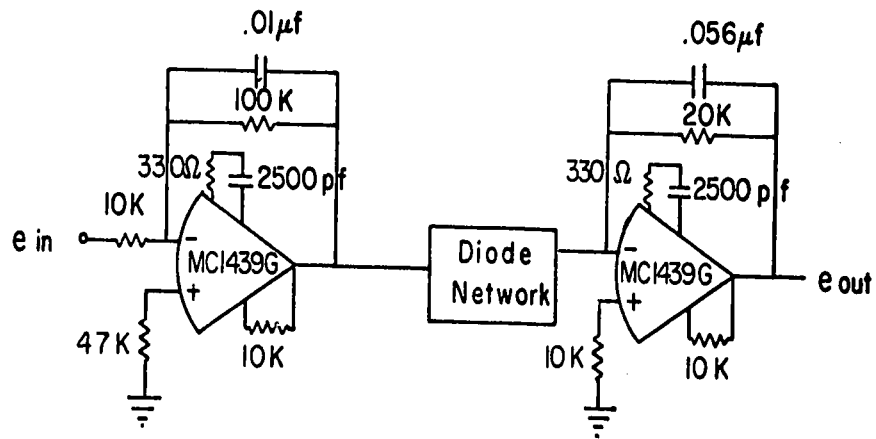Figure A-10. Square root circuit.

Figure A-11. Diode network.

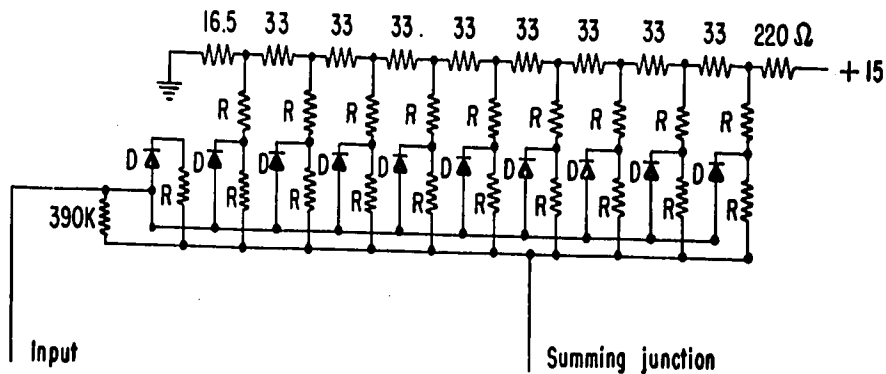Figure A-12. Squaring circuit and range control.

Figure A-13. Diode network.

A2.7 Meter Circuit

A meter (50 ma 0 - 50 ma) was used in the flow meter. It serves two functions; as a balancing meter for zero velocity and as a readout of flow rate. In the balance position the meter is connected to the output amplifier of the system (before the range switch). In the flow position the meter measures the linearized output voltage of the linearized output voltage of the system. The sensitivity of the meter is reduced with a series resistor so that 10 volts gives a full scale deflection.

A2.8 Power Supplies

The system requires ± 15 volt power supplies at 200 ma. Regulated power supplies were designed to provide ± 15 volts at 500 ma.